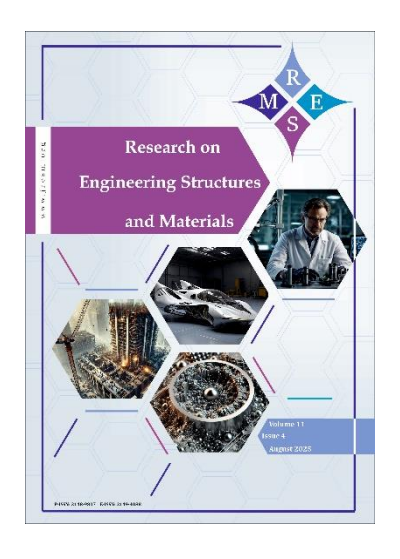


Research on Engineering Structures & Materials



www.jresm.org



Effects of pipe vibration on roll angle of a quadrotor system with a vertical cantilever pipe conveying fluid

Habibe Gursoy Demir

Online Publication Date: 20 June 2025

URL: http://www.jresm.org/archive/resm2025-898st0515rs.html

DOI: http://dx.doi.org/10.17515/resm2025-898st0515rs

Journal Abbreviation: Res. Eng. Struct. Mater.

To cite this article

Gursoy Demir H. Effects of pipe vibration on roll angle of a quadrotor system with a vertical cantilever pipe conveying fluid. *Res. Eng. Struct. Mater.*, 2025; 11(5): 1889-1912.

Disclaimer

All the opinions and statements expressed in the papers are on the responsibility of author(s) and are not to be regarded as those of the journal of Research on Engineering Structures and Materials (RESM) organization or related parties. The publishers make no warranty, explicit or implied, or make any representation with respect to the contents of any article will be complete or accurate or up to date. The accuracy of any instructions, equations, or other information should be independently verified. The publisher and related parties shall not be liable for any loss, actions, claims, proceedings, demand or costs or damages whatsoever or howsoever caused arising directly or indirectly in connection with use of the information given in the journal or related means.



Published articles are freely available to users under the terms of Creative Commons Attribution - NonCommercial 4.0 International Public License, as currently displayed at here (the "CC BY - NC").



Research on Engineering Structures & Materials



www.jresm.org

Research Article

Effects of pipe vibration on roll angle of a quadrotor system with a vertical cantilever pipe conveying fluid

Habibe Gursoy Demir a

Department of Aerospace Engineering, Iskenderun Technical University, Faculty of Aeronautics and Astronautics, Hatay, Türkiye

Article Info

Abstract

Article History:

Received 15 May 2025 Accepted 18 June 2025

Keywords:

Quadrotor; Pipe; Vibration analysis; Finite element method; Fluid conveying A quadrotor + liquid conveying pipe system is used to transport liquids in applications where direct human intervention is impractical, such as firefighting, precision agriculture, industrial maintenance and cleaning. While the quadrotor provides mobility, the pipe acts as a conduit for continuous liquid transport from a reservoir. In this study, the coupled dynamics between quadrotor system and a vertical cantilever pipe conveying fluid were investigated. For this purpose, a coupled model was developed by connecting the pipe and the quadrotor model. It was assumed that the pipe vibrations affect the quadrotor but not the other way around. The effects of fluid speed and distribution impacts based uncontrolled pipe vibrations on the uncontrolled and PD controlled quadrotor were determined. The results show that fluid speed and pipe excitation significantly affect the stability of the quadrotor and cause variations in the roll angle and displacement at the free end of the pipe. It is observed that the pipe vibration and the torque applied to the quadrotor decrease as the fluid speed is increased until the critical speed is reached. It is observed that the flow velocity and the type of disturbance excitation affect the time domain performance criteria of the roll angle.

© 2025 MIM Research Group. All rights reserved.

1. Introduction

Quadrotor systems have a wide range of applications in aviation and robotics and are widely used in search and rescue operations, military reconnaissance missions and data collection in disaster areas. These systems offer high maneuverability in narrow spaces and can perform reconnaissance and surveillance in dangerous areas without human intervention. In addition, thanks to advanced sensor and camera systems, they are also quite successful in tasks such as mapping, object tracking and environmental analysis. Due to these successes, one of the most important areas of use of quadrotors, which are used in many areas, is the use of liquid transfer and application situations that need to be applied remotely. For this purpose, a liquid tank that can be carried by the quadrotor system or a hose for pumping liquid from the ground can be added. With all these additions, the liquid must be sprayed with the help of a pipe to transfer the liquid to the relevant area. For this purpose, the dynamics of the pipe added to UAVs such as quadrotors and through which the liquid flows create an effect together with the dynamics of the quadrotor, and external effects on the quadrotor occur in addition to pipe vibrations.

Using a UAV with a liquid delivery pipe is a method that increases efficiency in applications, improves safety, and expands accessibility in situations where traditional liquid delivery methods are impractical. This type of UAV is an advanced airborne system designed to transport and distribute fluids during flight and is useful in a variety of applications such as firefighting [1],

 $Corresponding\ author: \underline{habibe.gursoydemir@iste.edu.tr}$

^aorcid.org/0000-0002-7705-9516

DOI: http://dx.doi.org/10.17515/resm2025-898st0515rs Res. Eng. Struct. Mat. Vol. 11 Iss. 5 (2025) 1889-1912

precision agriculture [2], window cleaning of high-rise buildings [3] and industrial inspections [4]. Another application area is the cleaning of solar panels with water at a certain interval as their efficiency decreases as they get dirty. As seen in these application areas, UAVs connected to a land-based fluid source in particular guarantee continuous operation, reduce intervention time and provide time and cost savings while increasing occupational safety. In addition, these types of UAVs optimize resource use in all applications while minimizing environmental impact. They can reduce human exposure to hazardous conditions by transporting coolants, lubricants or decontaminants to remote machines, chemical spill areas or biohazard zones.

Generally, studies on this subject are focused on design and implementation, and these studies generally focus on UAVs with robot manipulators. There is one study in the literature where fluidconveying pipes are integrated into the UAV. Lee et al. [5] investigated the effects of fluid-structure interaction (FSI) on the stability of a quadrotor when it is connected to a flexible hose that exhausts pressurized fluid. They derived an analytical solution to analyze the free-end response of the hose that affects the UAV stability. However, modeling of UAVs with manipulators in the literature is like this study due to the interaction between the UAV and the manipulator. Therefore, in the introduction section, we focused on modeling and analysis studies on UAVs with manipulators and vibration of fluid-conveying pipes. Omar and Mukras [6] presented a multi-rotor flying vehicle equipped with a crane and robotic arm to increase the efficiency and safety of date palm harvesting. Remotely controlled via a mobile app with live video feedback, the system cuts branches with precision, reducing reliance on dangerous traditional methods. A decoupled control scheme for an aerial manipulator consisting of a UAV and two robotic arms has been presented by Ruiz et al. [7]. Simulations confirm the ability of the system to perform complex tasks while maintaining synchronization with a predetermined audio signal, and the success of the controller implemented in structured aerial environments providing precise coordination between the UAV and the robotic arms has been demonstrated. A novel end effector mechanism designed to grasp and then place or throw objects using stored elastic energy was presented by Pasala et al. [8]. A mechanical design, simulation model and data-driven residual learning framework are developed to improve launch accuracy despite model uncertainties. Experiments are conducted to demonstrate the effectiveness of the end effector and algorithms for targeted launch. Choi and Jung [9] studied experimental studies on solar panel cleaning using a drone manipulator. A foldable and lightweight drone arm was designed that included a flexing mechanism to suppress vibration and hybrid force control to regulate contact force. Clustering algorithms were used to classify cleaning areas and efficient cleaning performance was achieved. In another application, Raj et al. [10] designed an autonomous drone with a robotic arm on top to inspect and repair faults in mobile towers. In this study, they developed an innovative matching algorithm that allows the drone to stabilize with less energy while the arm performs repair tasks. Suarez et al. [11] analyzed benchmarks for aerial manipulation robots performing physical interactions in high altitude workspaces. Various evaluation methods and criteria were defined to compare the performance considering different designs and applications, and experimental results obtained with a compliant joint aerial manipulator were compared for accuracy, execution time, manipulation ability, and impact response. Mendoza-Mendoza et al. [12] designed a new aerial manipulator based on multirotors, which uses yaw motion to generate and transmit forces through a serial chain of rigid links and drones. The experimental data were compared with existing technologies. They provided suggestions for further development along with potential application examples highlighting the scientific and social impact of the system. Readers who need more information on modeling, design, and applications of drones with robot manipulators can refer to the review works of Ramalepa and Jamisola [13] and Saunders et al. [14]. Ramalepa and Jamisola focused on collaborative robotic arms with fixed, mobile or drone bases to increase efficiency and safety [13]. They discussed the application areas of these robots, areas where they increase their efficiency, and collision avoidance, path planning and control.

Saunders et al. [14] reviewed research problems and state-of-the-art solutions for package delivery using aerial manipulators and grippers. The challenges associated with landing on both static and dynamic platforms were discussed, and risks such as weather conditions, attitude estimation and collision avoidance were examined. Another subsystem that needs to be addressed in accordance

with the content of the study is the fluid-conveying pipes. The dynamics and vibration analyses of these systems under different conditions are of great importance in terms of the effects they will have on the entire system. Fluid-conveying pipes are essential components of various engineering applications that facilitate the controlled [18] transportation of liquids and gases in industries such as oil and gas [15], water supply, chemical processing [16] and aviation [17]. These pipes play an important role in maintaining efficiency, safety and reliability in systems that require precise fluid transport at different pressures and temperatures. Advances in materials, design and monitoring technologies continue to increase their durability and performance, making them indispensable in modern engineering infrastructure.

Although generally perceived as static elements, these pipes are inherently dynamic systems that can exhibit complex vibration behaviors when subjected to dynamic interactions with the fluid in transit, external forces applied by supporting structures, or disturbances from the surrounding environment. Vibration in fluid-conveying pipes can be defined as the oscillatory motion of the pipe structure resulting from dynamic interactions with the fluid in transit, external forces applied by supporting structures, or disturbances from the surrounding environment. This phenomenon arises from the continuous and flexible nature of the pipe as a mechanical system. The primary source of vibration in fluid-conveying pipes is the dynamic interaction between the fluid flow and the pipe structure. This interaction is complex in nature and is influenced by a multitude of factors, including the velocity, density, and viscosity of the fluid, as well as the material properties, geometric configuration, and support conditions of the pipe. One of the primary mechanisms by which fluid flow causes vibration is the generation of inertial forces, particularly Coriolis and centrifugal forces. This complex relationship between fluid flow and the pipe structure brings fluidstructure interaction (FSI) to the forefront in the context of fluid-conveying pipe vibrations. This relationship between the fluid and the liquid has been addressed in the literature under many conditions and dynamic and vibration analyses of the fluid conveying pipe have been carried out. Detailed initial studies for modeling and dynamic examination of these systems have been made by Paidoussis and Issid [19] and Paidoussis and Li [20]. In these studies, the dynamics of the fluid conveying pipes have been examined and the extensive research carried out in this field has been emphasized. Various aspects including different boundary conditions, fluid types and linear or nonlinear behaviors have been analyzed. In these studies, it has been shown that the system exhibits complex dynamic behavior, and it has been stated that it is possible to examine it from both structural and control perspectives. Since the focus of the study is on the integration of the cantilever pipe to the quadrotor, the studies on the dynamic analysis of the cantilever pipe have been reviewed below.

Modarres-Sadeghi et al. [21] investigated the two-dimensional (2-D) and three-dimensional (3-D) fluttering of fluid-conveying cantilever pipes using a full set of nonlinear equations of motion. The stability behavior of horizontal and vertical systems was analyzed considering the effects of increasing flow velocity beyond the Hopf bifurcation. Liu et al. [22] presented a comprehensive study on the planar oscillations of a cantilever pipe conveying fluid under bottom excitation. The effects of flow velocity, excitation frequency and amplitude on the dynamic response of the pipe were investigated. Li et al. [23] proposed a feedforward vibration suppression method for fluidconveying cantilever pipes. The dynamic equation was established using the Euler-Bernoulli beam model, and the vibration function of pipeline pressure was formulated by Fourier series to analyze the transient response. The effectiveness of optimizing the input signal parameters to minimize tip vibration was demonstrated through theoretical derivation and experimental verification. The dynamics of thin cantilever cylinders, plates and pipes subjected to internal or external axial flow have been studied extensively since the 1960s by Paidoussis [24]. The differences in behavior between conventional and reversed axial flow were analyzed and it was shown that reversed flow leads to weak flutter at low speeds and large amplitude static deflection at higher speeds. Semler and Paidoussis [25] investigated the nonlinear dynamics and stability of cantilever pipes conveying harmonic component fluid placed on a constant mean velocity. In this work, the effects of forcing frequency, disturbance amplitude and flow velocity on the pipe dynamics were analyzed, especially near the critical flutter instability. Some of the studies related to dynamic analysis of cantilever pipes are summarized and for more detailed information, readers can refer to references [26-30]. In addition, as seen in these studies, studies are carried out using both active and passive elements to cause vibrations in the pipe and to damp these vibrations. For this purpose, there are many studies in the literature using methods and equipment such as electromagnetic actuators [31], eddy-current dampers [32], mass dampers [33], piezoelectric actuators [34], artificial neural network-based control technique [35], adaptive modal control technique [36], feedforward control strategy based [37], LQR control technique [38], nonlinear energy sink [39] and feedback coupling [40]. The readers refer the review paper [41] for more details about control of the pipe vibration.

In this study, modeling and dynamic analysis of a vertically cantilever pipe connected quadrotor system will be performed based on the Euler and Euler-Bernoulli techniques for quadrotor and fluid conveying pipe, respectively. This paper extends the previous paper by adding coupled model between the quadrotor dynamics and fluid conveying pipe dynamics. The coupled model is developed in which the motion of the pipe affects the motion of quadrotor. Quadrotor+Pipe system, while spraying the liquid fed by the pump from the ground to a certain area, the effects of the pipe vibrations on the motion dynamics of the quadrotor will be examined in detail. The pipe vibrations and roll angle of the quadrotor are observed under controller, different fluid speed and different distribution impacts on the free end of the pipe such as unit step and sinusoidal inputs within a certain time period.

2. Mathematical Modelling

Quadrotor is a type of unmanned aerial vehicle with four rotors that provide lift, balance and precision maneuverability. It is widely used in various areas such as surveillance, delivery, agriculture and infrastructure maintenance with its ability to hover in the air, navigate in narrow areas and operate autonomously. In recent years, quadrotors have become frequently preferred due to their advantages in terms of cost, work safety and time, as they can perform tasks efficiently and safely in dangerous or hard-to-reach areas without requiring human intervention. For this purpose, they have begun to be frequently preferred in applications such as cleaning solar panels, irrigation or spraying from agricultural applications and remote intervention in fires.

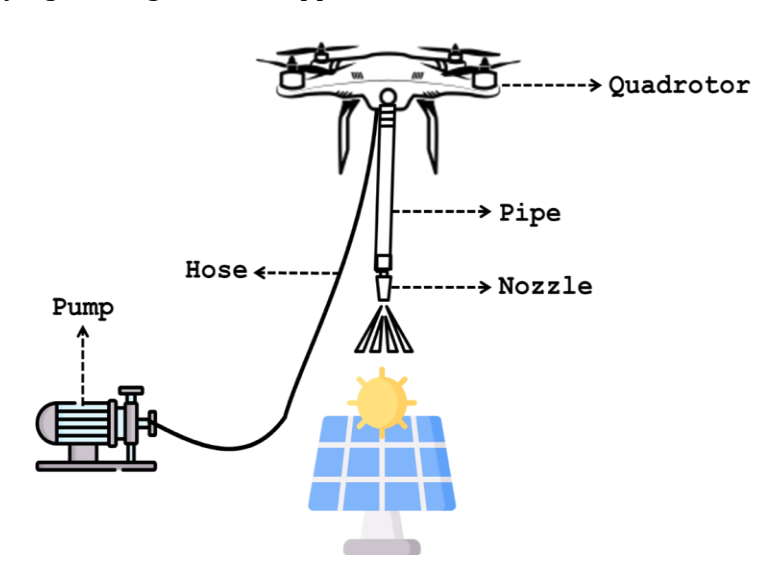


Fig. 1. The schematic diagram of Quadrotor+Pipe system

In all these applications, the liquid to be transferred is transferred via a pipe. This pipe is attached to the bottom of a quadrotor and is fed either from a tank mounted on the quadrotor or from a tank on the ground via a pump and hose. Since the liquid passing through this pipe flows in a non-uniform structure while being transferred, it causes vibrations in the pipe. These vibrations in the pipe cause the bending moment and force to occur at the point where the pipe is connected to the quadrotor, and the effects on the quadrotor also occur depending on the vibrations in the pipe. In order to analyze all this movement, the dynamics of the quadrotor and the fluid-conveying pipe were considered in this study. Then, a coupled model was created that combined these two dynamics. Figure 1 shows the schematic of the quadrotor+pipe system created in this study.

2.1. Quadrotor

The dynamics of a quadcopter include the mathematical and physical principles that govern its motion. These dynamics are based on aerodynamics to provide lift, steering and stability. For this reason, the motion of the quadrotor is modeled through translational and rotational motions affected by the forces and torques produced by the four rotors. Each of the four rotors is independently accelerated or decelerated to move in different directions. The basic motions of the quadrotor consist of four main parts: ascent-descent (thrust), forward-backward motion (pitch), right-left motion (roll) and rotation around its own block (yaw). The dynamic model is obtained using the Newton-Euler equations and this model determines the response of the system according to the force and torque balances. Figure 2 shows a schematic of a quadrotor and the forces and moments acting on it. Before calculating the dynamics of the quadrotor, some assumptions are needed to simplify the mathematical complexity [42].

- UAV structure and propellers are rigid and symmetrical
- Center of mass and body fixed frame origin are assumed to coincide with each other
- Thrust and drag are proportional to the square of the propeller speed
- Inertia matrix is time invariant.

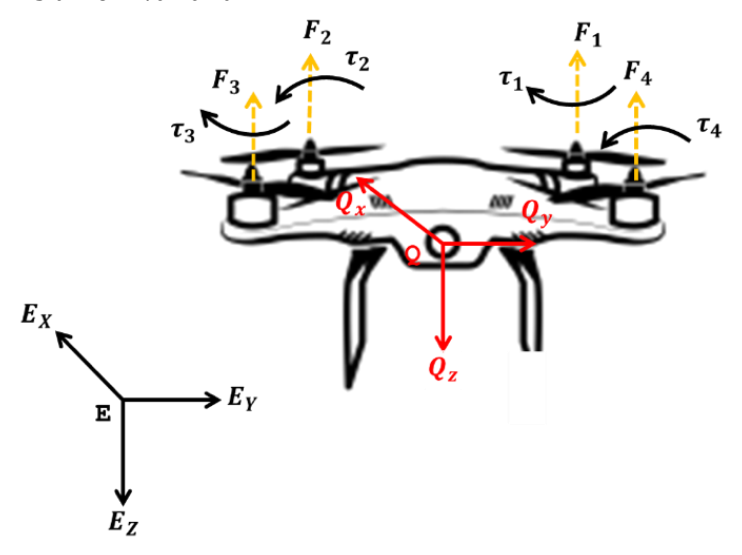


Fig. 2. The model of quadrotor system

As can be seen from the figure, the quadrotor has coordinated systems on the Earth and on itself. For this reason, the rotation matrix (R) is used to convert the observed motion on the Earth into the motion in the coordinate system on itself.

$$\begin{bmatrix}
\dot{X} \\
\dot{Y} \\
\dot{Z}
\end{bmatrix} = R \begin{bmatrix} U \\ V \\
W \end{bmatrix}$$

$$R = R_x R_y R_z = \begin{bmatrix}
\cos \psi \cos \phi & \cos \psi \sin \theta \sin \phi & \cos \psi \sin \theta \cos \phi + \sin \psi \sin \phi \\
\sin \psi \cos \theta & \sin \psi \sin \theta \cos \phi - \sin \phi \cos \phi \\
-\sin \theta & \cos \theta \sin \phi & \cos \theta \cos \phi
\end{bmatrix}$$
These equations, X, Y and Z indicate the position of the quadrotor on the Earth coordinate system. And W indicate the position of the quadrotor with respect to its own coordinate system. In the

In these equations, X, Y and Z indicate the position of the quadrotor on the Earth coordinate system. U, V and W indicate the position of the quadrotor with respect to its own coordinate system. In the equation, ϕ represents the roll angle, θ represents the pitch angle, and ψ represents the yaw angle. In this case, the dynamic equations of the quadrotor are given below. The readers looking for detailed information on modeling can refer to references [43] and [44].

$$\ddot{x} = -\frac{1}{M_{auad}} (u_1(\sin\varphi\sin\phi + \cos\varphi\cos\varphi\sin\theta)) \tag{3}$$

$$\ddot{y} = -\frac{1}{M_{quad}} (u_1(cos\varphi sin\phi - cos\phi sin\varphi sin\theta)) \tag{4}$$

$$\ddot{z} = \frac{1}{M_{quad}} \left(-M_{quad}g + u_1 cos\phi cos\theta \right) \tag{5}$$

$$\ddot{z} = \frac{1}{M_{quad}} (-M_{quad}g + u_1 cos\phi cos\theta)$$

$$\begin{bmatrix} \dot{p} \\ \dot{q} \\ \dot{r} \end{bmatrix} = \begin{bmatrix} I_{xx} & 0 & 0 \\ 0 & I_{yy} & 0 \\ 0 & 0 & I_{zz} \end{bmatrix}^{-1} + \begin{pmatrix} -\begin{bmatrix} p \\ q \end{bmatrix} x \begin{bmatrix} I_{xx} & 0 & 0 \\ 0 & I_{yy} & 0 \\ 0 & 0 & I_{zz} \end{bmatrix} \begin{bmatrix} p \\ q \end{bmatrix} + \begin{bmatrix} u_2 \\ u_3 \\ u_4 \end{bmatrix}$$

$$\dot{q} = n + r \cos\phi t an\theta + a \sin\phi t an\theta$$
(5)

$$\dot{\phi} = p + r\cos\phi \tan\theta + q\sin\phi \tan\theta \tag{7}$$

$$\dot{\theta} = q\cos\phi - r\sin\phi \tag{8}$$

$$\ddot{\varphi} = \frac{r\cos\phi}{\tan\theta} + \frac{q\sin\phi}{\cos\theta} \tag{9}$$

In these equations, u_i (i = 1,2,3,4) shows the thrust force applied to the quadrotor system because of the rotation of the rotors and the moments that lead to Euler angular movements. These effects occur due to the rotation of the rotors depending on the voltage supply. For this reason, there is a connection between the angular velocities of the motors and the forces and moments generated.

$$\begin{bmatrix} u_1 \\ u_2 \\ u_3 \\ u_4 \end{bmatrix} = \begin{bmatrix} F_1 + F_2 + F_3 + F_4 \\ F_4 - F_2 \\ F_3 - F_1 \\ F_2 + F_4 - F_3 - F_1 \end{bmatrix} = \begin{bmatrix} b(w_1^2 + w_2^2 + w_3^2 + w_4^2) \\ b(w_4^2 - w_2^2) \\ b(w_3^2 - w_1^2) \\ d(-w_1^2 + w_2^2 - w_3^2 + w_4^2) \end{bmatrix}$$
(10)

 F_i (i = 1,2,3,4) forces seen Eq. (10) represent the forces produced by the rotors shown in Figure 2. The b and d parameters show the thrust and drag constants. These constants were determined under certain conditions and were taken constant throughout the study.

2.2. Fluid Conveying Cantilever Pipe

In the system under consideration, in addition to the quadrotor, a uniform vertical suspended pipe of length L and mass per unit length M_{fluid} and an incompressible fluid of axial velocity u and mass per unit length M_{pipe} are included. For the vertical suspended pipe, the z axis is in the direction of gravity and the y axis is the horizontal axis to be suitable for the quadrotor system. In the system under consideration, in addition to the quadrotor, a uniform vertical suspended pipe of length L and mass per unit length M_{fluid} and an incompressible fluid of axial velocity u and mass per unit length M_{pipe} are included.

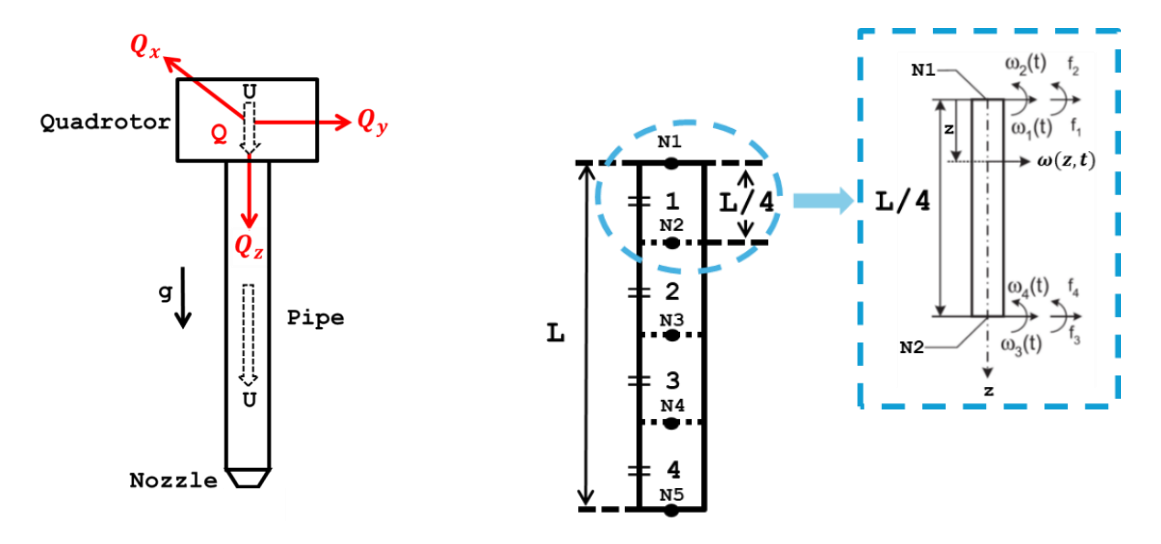


Fig. 3. The scheme of fluid conveying pipe

Fig. 4. Finite element model of the pipe and the applied forces on each element

For the vertical suspended pipe, the z axis is in the direction of gravity and the y axis is the horizontal axis to be suitable for the quadrotor system. A schematic representation of the pipe used in the system is given in Figure 3.

In this system, it can be assumed that the pipe free movements occur in the (y-z) plane and all movements are small. y(z,t) represents the transverse deviation of the pipe from its equilibrium position. Other assumptions made to determine the forces acting on the pipe and the fluid motion are: i) the pipe does not change its shape due to pressure ii) the pipe material is elastic and linear. The equation of motion for the free transverse vibration of a vertically suspended pipe for different boundary conditions was obtained by Paidoussis and Issid [19] using the Newtonian approximation.

$$E^*I \frac{d^5y}{dz^4dt} + EI \frac{d^4y}{dz^4} + M_{pipe}uU_j \frac{d^2y}{dz^2} - (M_{pipe} + M_{fluid})g \frac{d^2y}{dz^2}(L-z) + M_{pipe} \frac{du}{dt}(L-z) \frac{d^2y}{dz^2} + 2M_{pipe}u \frac{d^2y}{dzdt} + (M_{pipe} + M_{fluid})g \frac{dy}{dz} + c \frac{dy}{dt} + (M_{pipe} + M_{fluid}) \frac{d^2y}{dt^2} = 0$$
(11)

In Eq. (11), E is the elastic modulus of the pipe, and I is the sectional moment of inertia of the pipe. E* represents the internal damping coefficient of the pipe material, and this material is assumed to be Kelvin-Voigt type viscoelastic. c represents the viscous damping coefficient due to the friction of the pipe with the surrounding stationary fluid medium, and g represents the gravitational acceleration. In this study, it is additionally assumed that the fluid flowing in the pipe has harmonics and that there is a nozzle at the end of the pipe that increases the exit velocity of the fluid. The flow rate is assumed to be in the form $U_0=u(1+\mu\cos\cos(w_dt))$). Here u is the average flow rate, μ is the amplitude of the added harmonic component and is assumed to be less than 1. w_d is the circular frequency. When it comes to the nozzle part, the weight of the nozzle is assumed to be small enough to be neglected and its length is quite short compared to the total length of the pipe. The exit speed is calculated with the formula $U_j = U_0 * A_1/A_2$. A_1 represents the cross-sectional area of the pipe and A_2 represents the nozzle exit area. Boundary conditions are needed to solve the general differential equation for pipe vibration given in Eq. (11). General boundary conditions for a fixed pipe are given in Eq. (12). The correct application of boundary conditions in cantilever beams is critical for the stability and convergence of the solution. While correct boundary conditions both increase accuracy and shorten the computational time, missing or excessive constraints can negatively affect the results. Therefore, boundary conditions that best reflect the physical situation and restrict only the necessary degrees of freedom were preferred.

$$y(0,t) = \frac{d^2y(0,t)}{dz^2} = 0 , z = 0$$

$$\frac{d^2y(L,t)}{dz^2} = \frac{d^3y(L,t)}{dz^3} = 0 , z = L$$
(12)

Finite element analysis is used to solve the equation given by Eq. (11) with boundary conditions. In this analysis, firstly the main differential equation is discretized using the weak formulation. As shown in Figure 4, the cantilever pipe system is divided into four equal parts and contains a total of five nodes. Using more beam elements in FEM analysis provides more accurate modeling of structural behavior, especially in regions with high stress or displacement gradients. As the number of elements increases, the numerical solution gets closer to the analytical (real) solution and the quality of convergence increases. However, one of the disadvantages of using more elements is the increase in solution time and effort. This process increases the degrees of freedom and causes the system matrices to grow. Fine meshes that increase sensitivity are useful, but a balanced mesh structure should be preferred to avoid unnecessary computational load. For this reason, it was found appropriate to choose 4 elements for the pipe. According to the finite element method, these nodes of each element undergo both linear $(\omega_1(t))$ and $\omega_3(t)$ and rotational $(\omega_2(t))$ and $\omega_4(t)$ displacements. The linear joint forces $f_1(t)$ and $f_3(t)$ correspond to linear displacements, and the rotational joint forces $f_2(t)$ and $f_4(t)$ correspond to rotational displacements. In Figure 4, the forces and displacements of a pipe element of length L/4 are clearly shown. The system solution obtained using the weak formulation of the finite element method is obtained with the formula in Eq. (13). In this equation, $W_i(t)$ and $N_i(z)$ express the displacement and shape functions.

$$y(z,t) = \omega(z,t) = \sum_{i=1}^{4} W_i(t) N_i(z)$$
 (13)

It is extremely important to determine the shape functions that help to interpolate the variable values between two different nodes having discrete values of the variable, by considering that their derivatives can be taken depending on the boundary conditions. The selection of shape functions in FEM analysis directly affects the accuracy, convergence and computational efficiency of the solution. In order to obtain accurate results, it is important to use higher order shape functions, but higher order functions require more computational resources. In addition, appropriate shape functions provide faster convergence of the solution to the real solution as the mesh becomes thinner. For this reason, a balance must be established between accuracy and efficiency, and the differentiability and applicability of shape functions should not be controlled depending on the boundary conditions. For this reason, the shape function are determined as follows.

$$N_{1}(z) = 1 - 3\left(\frac{z}{l}\right)^{2} + 2\left(\frac{z}{l}\right)^{3}$$

$$N_{2}(z) = z - 2l\left(\frac{z}{l}\right)^{2} + l\left(\frac{z}{l}\right)^{3}$$

$$N_{3}(z) = 3\left(\frac{z}{l}\right)^{2} - 2\left(\frac{z}{l}\right)^{3}$$

$$N_{4}(z) = -l\left(\frac{z}{l}\right)^{2} + l\left(\frac{z}{l}\right)^{3}$$
(14)

At the end of the finite element method, the mass, gyroscopic and stiffness matrices obtained for each element of the system are obtained and the displacements of each mode can be obtained by using Eq. (15).

$$M_e \ddot{\omega}(z,t) + G_e \dot{\omega}(z,t) + K_e \omega(z,t) = 0 \tag{15}$$

The mass, gyroscopic and stiffness matrices of each element seen in this equation are given in the Appendix. After this process, the matrices obtained for each element are combined to obtain the general equation of motion. Global matrices are obtained by combining the element matrices by applying the matrix operations given in Eq. (16) and then deleting the appropriate rows and columns in line with the boundary conditions.

$$M = \sum_{s=1}^{p} A_s^T M_e A_s \qquad , \qquad G = \sum_{s=1}^{p} A_s^T G_e A_s \qquad , \qquad K = \sum_{s=1}^{p} A_s^T K_e A_s$$
 (16)

where A_s is rectangular matrix with four rows and its column number is equal to the selected number of joints displacements in the global coordinate system. General equation of motion is

$$M_G \ddot{w}(z,t) + G_G \dot{w}(z,t) + K_G w(z,t) = F = F_C + F_{ext}$$
 (17)

where F_c and F_{ext} denote the control and external inputs, respectively. F_{ext} consists of the external forces (F_d) and the forces (F_{quad}), which is applied by the motion of the quadrotor.

2.3. Coupled Model

The system consisting of a quadrotor and a fluid conveying pipe provides the relationship between each other with the forces and moments created by both the quadrotor and the pipe on each other. The pipe applies a force and moment on the quadrotor at the connection point and these forces and moments change depending on the vibration of the pipe. The quadrotor creates inertial forces on the pipe due to translational and rotational accelerations depending on its movement. In addition, since the center of mass of the two interconnected systems shifts to different places, this causes a disruptive external effect on the vibrations of the pipe. However, since the movements of the quadrotor are assumed to be quite small in this study, the effect of the change of the center of mass is neglected.

The first part of this coupled equation of motion is the bending force and moment transferred by the pipe to the quadrotor. For this purpose, the force and moment at point z=0 are obtained using the following equations.

$$M(x) = EI\left(\frac{d^2w}{dz^2}\right) = EI\left(\frac{d^2N}{dz^2}\right) \begin{cases} \omega_1(0,t) \\ \omega_2(0,t) \\ \omega_3(0,t) \\ \omega_4(0,t) \end{cases}$$
(18)

As can be seen here, since the second derivatives of the shape functions are linear, the bending moment M(y) is also obtained linearly. Similarly, the shear force (V(y)) is also obtained as a constant since the third derivatives of the shape functions are constant.

$$V(x) = EI\left(\frac{d^3w}{dz^3}\right) = EI\left(\frac{d^3N}{dz^3}\right) \begin{cases} \omega_1(0,t) \\ \omega_2(0,t) \\ \omega_3(0,t) \\ \omega_4(0,t) \end{cases}$$
(19)

By using these two equations, the equations between Eq. (3) and Eq. (5) are rewritten as follows. In this equation, the force V(y) acts in the y-direction and the weights of the pipe, fluid and hose act in the z-direction.

$$M_{total} \begin{bmatrix} \ddot{x} \\ \ddot{y} \\ \ddot{z} \end{bmatrix} = Ru_1 - M_{total} g \hat{e}_z + V(y) \hat{e}_y$$
 (20)

$$M_{total} = M_{quad} + M_{pipe} + M_{fluid} + M_{hose}$$
(21)

where M_{hose} denotes the mass per unit length of the hose. Moreouver, $\widehat{e_y}$ and $\widehat{e_z}$ are the unit vectors along the y axis and z axis, respectively. Similarly, the bending moment exerted by the pipe also affects the Euler angles of the quadrotor. The Eq. (6) changes to the following general form.

$$I_{total} \begin{bmatrix} \ddot{\phi} \\ \ddot{\theta} \\ \ddot{\psi} \end{bmatrix} = - \begin{bmatrix} \phi \\ \theta \\ \psi \end{bmatrix} x I_{total} \begin{bmatrix} \phi \\ \theta \\ \psi \end{bmatrix} + \begin{bmatrix} u_2 \\ u_3 \\ u_4 \end{bmatrix} + M(y) \begin{bmatrix} 1 \\ 0 \\ 0 \end{bmatrix}$$
 (22)

$$\begin{bmatrix} \dot{p} \\ \dot{q} \\ \dot{r} \end{bmatrix} = \begin{bmatrix} I_{xx} & 0 & 0 \\ 0 & I_{yy} & 0 \\ 0 & 0 & I_{zz_{total}} \end{bmatrix}^{-1} + \left(-\begin{bmatrix} p \\ q \\ r \end{bmatrix} x \begin{bmatrix} I_{xx} & 0 & 0 \\ 0 & I_{yy} & 0 \\ 0 & 0 & I_{zz_{total}} \end{bmatrix} \begin{bmatrix} p \\ q \\ r \end{bmatrix} + \begin{bmatrix} u_2 - M(y) \\ u_3 \\ u_4 \end{bmatrix} \right)$$
(23)

$$I_{zz_{total}} = I_{zz} + I_{pipe} + I_{hose} \tag{24}$$

The expressions $I_{zz_{total}}$ and I_{zz} in the equations show the total moment of inertia in the z direction and the 3x3 dimensional moment of inertia matrix in all directions, respectively. In addition, in this study, the effect of pipe vibrations on the quadrotor fixed at a certain height was investigated. For this reason, the movements of the quadrotor are very small and the effects it creates on the pipe are assumed to be very small. In this case, it is assumed that the quadrotor does not create any force on the pipe dynamics. Then, the general equation of motion of the fluid-conveying pipe given in Eq. (17) can be rewritten as follows.

$$M_G \ddot{w}(z,t) + G_G \dot{w}(z,t) + K_G w(z,t) = F = F_c + F_d \text{ and } F_{quad} = 0$$
 (25)

4. Results and Discussion

In this study, the quadrotor system is combined with a vertical pipe conveying fluid and the dynamics of this general system are investigated. In the considered system, the effects of pipe vibrations on the quadrotor are investigated for different conditions. The pipe vibrations and the effects of these vibrations on the quadrotor are discussed in detail for different fluid velocities and pipe-fluid parameters. Since the pipe is in the z direction and the pipe vibrations create a displacement in the x direction, it is assumed that all movements of the fluid-conveying pipe are in the x-z plane. For this reason, the effects of the displacements in the pipe, the shear force at the z=0

point and the bending moment at the same point on the quadrotor are in different directions. While the shear force caused by the pipe vibrations affects the movement of the quadrotor along the x-axis, the bending moment affects the roll rotation around the y-axis.

Based on these explanations, it is seen that pipe vibrations affect only the roll motion of the quadrotor. In the tests, the change in roll motion was observed for different pipe impulses. The parameter values used for the pipe, fluid and quadrotor during the process of obtaining the results are given in Table 1 and Table 2.

Table 1. The parameters of the quadrotor

Properties	Value
M _{quad} (kg)	1.2
l (m)	0.23
I_{xx} (kg. m ²)	2.353×10^{-3}
I_{yy} (kg. m ²)	2.353×10^{-3}
I_{zz} (kg. m ²)	5.262×10^{-2}

Table 2. The physical properties of the pipe, fluid and hose

Properties	Value	Properties	Value
M _{pipe} (kg/m)	0.1064	$I = I_{pipe} + I_{hose} (kg. m^2)$	8.97×10^{-9}
M_{fluid} (kg/m)	0.0152	L (m)	3.2
M_{hose} (kg/m)	0.0842	A_{j}	2
E (Pa)	6.89×10^{10}		

In the tests performed, observations were made by applying disturbing impulses to the pipe after the quadrotor reached a certain height. Initially, an impulse was applied to the free end of the pipe for 1.5 seconds, lasting 0.05 seconds, without any control applied to the quadrotor. As a result, the roll motion of the quadrotor without any control was observed. Figure 5 shows the roll angle change of the quadrotor for different fluid velocities. As can be seen in these results, the vibrations occurring in the pipe due to the impulse cause instability in the roll motion even if the pipe is structurally damped. Figure 6 shows the pipe vibration under this impact for different fluid speeds. This shows that it would be easier to observe the effect of pipe vibrations on the roll motion by applying a simple controller to the quadrotor.

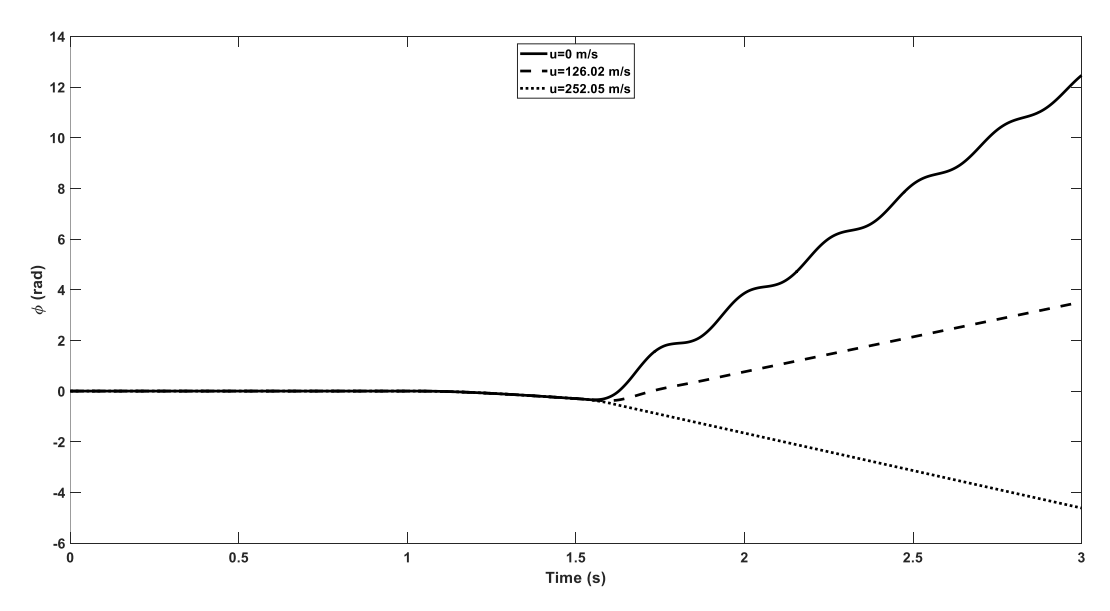


Fig. 5. Roll motion of uncontrolled quadrotor under pipe vibration at different fluid flow speeds

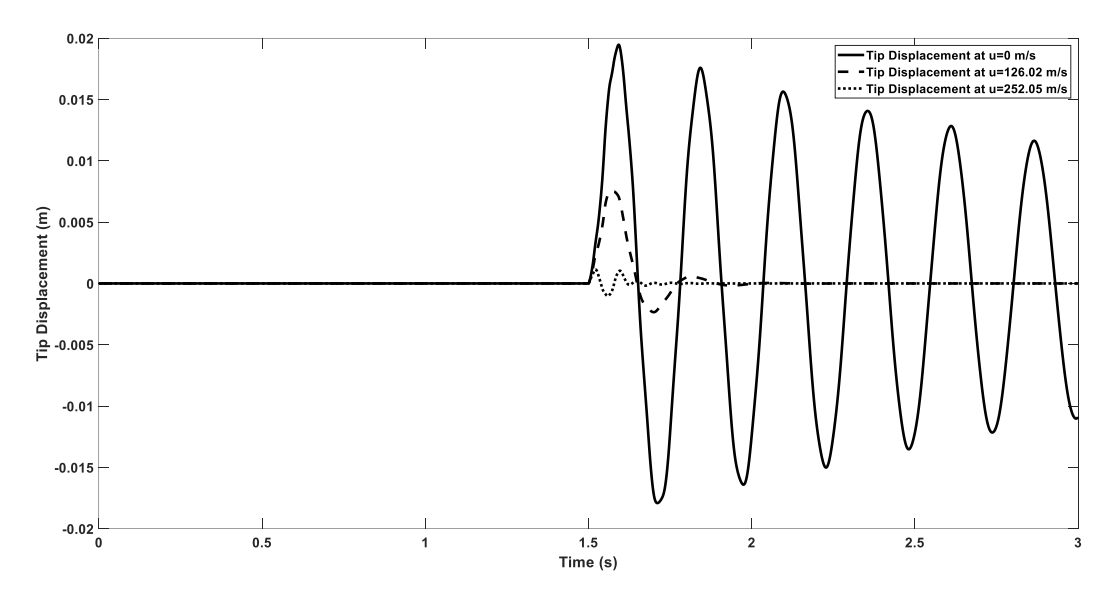


Fig. 6. Tip displacement of pipe at different fluid flow speeds

For this reason, a PD controller was designed to control the roll motion of the quadrotor. The primary reason for choosing PD control is that it is a simple and applicable controller. It also offers a good balance between speed and stability, making it ideal for dynamic systems that require fast response and reduced overshoot without the complexity of integral control. his controller has two basic control parameters: proportional gain (K_p) and derivative gain (K_d) . While K_p directs the system according to the current error, K_d responds to the rate of change of the error, reducing oscillations and making the system more stable. The K_p value was selected as 0.8 and the K_d value as 0.4 for the PD controller. The selection of these controller values was made by trial and error. Because the situation observed in this study is the effects of pipe vibrations on the dynamics of the quadrotor rather than the control of the roll motion. Therefore, it is sufficient for the roll motion to reach the reference value within the desired time interval.

4.1. Test Scenario 1

In this scenario, the effect of an impulse acting on the free end of the fluid-conveying pipe after the reference value of the roll motion of the quadrotor has been reached under the PD controller has been investigated. For this, the unit step acting on the free end has been effective for 0.1 seconds.

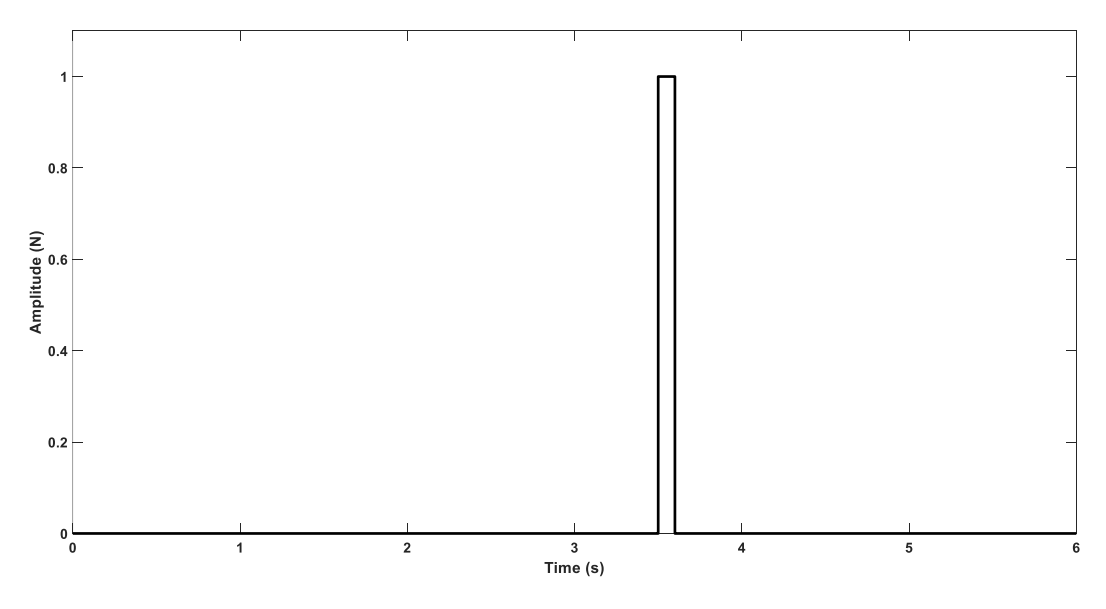


Fig. 7. The variation of the acting force at the free end of the pipe in Scenario 1

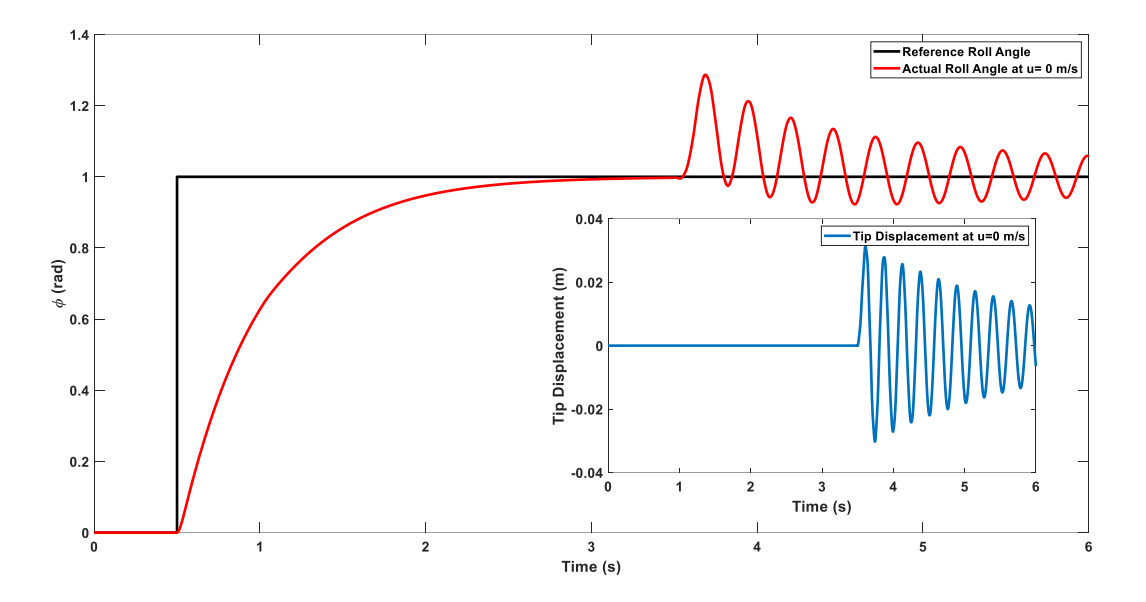
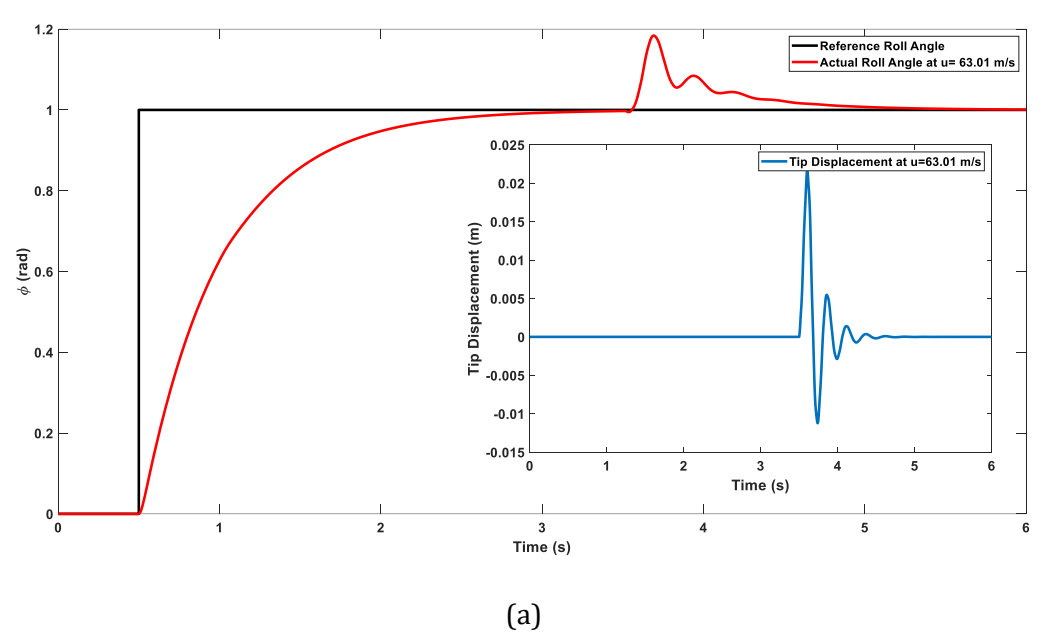
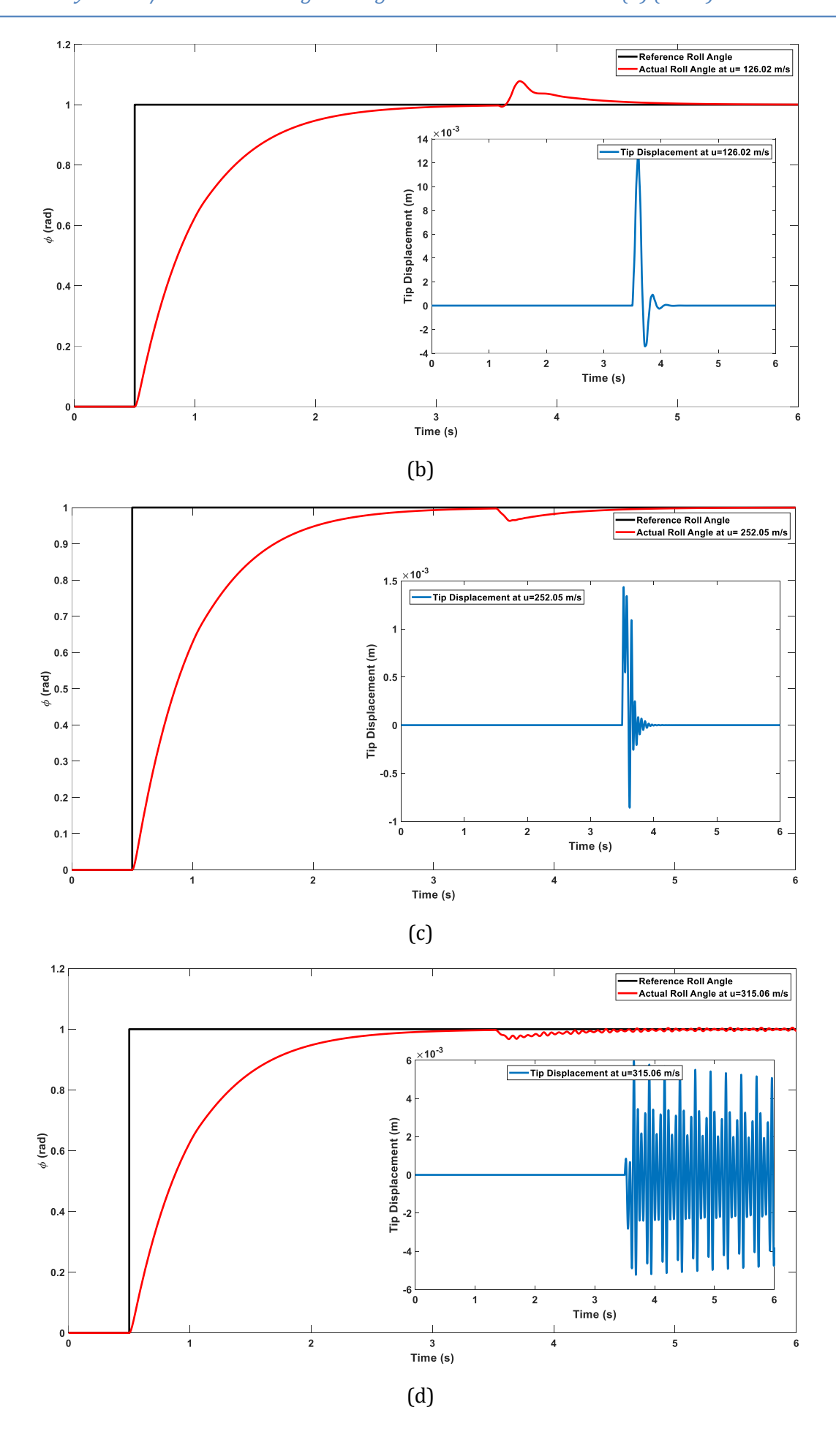


Fig. 8. Roll angle of PD controlled quadrotor under pipe vibration at u=0 m/s

The effect time of this impulse started at the t=3.5 sec of the movement. The acting force at the free end of the pipe is shown in Figure 7. Accordingly, the roll motion of the quadrotor, the free end vibrations of the pipe and the performance of the PD controller are observed in the following figures. Figure 8 shows the variation of the roll angle of quadrotor and the variation of the tip displacement of pipe when the fluid flow speed is 0 m/s. At this fluid velocity, the pipe behaves like a cantilever beam. The results show that the pipe oscillates for a long time in response to the applied force, which causes oscillation in the roll motion. The controller also takes time to dampen this oscillation, depending on the pipe vibrations. By designing a more successful controller, this damping time can be shortened, and thus, the vibrations of a pipe without fluid can be ensured to have a minimum effect on the quadrotor motion.

In Figure 9, the roll response of the quadrotor under this input effect is observed for different fluid velocities. The fluid velocity inside the pipe varies between 63 m/s and 346.57 m/s. At these velocities, the roll movement and pipe end displacement resulting from the disturbing effect applied to the free end of the pipe were observed.





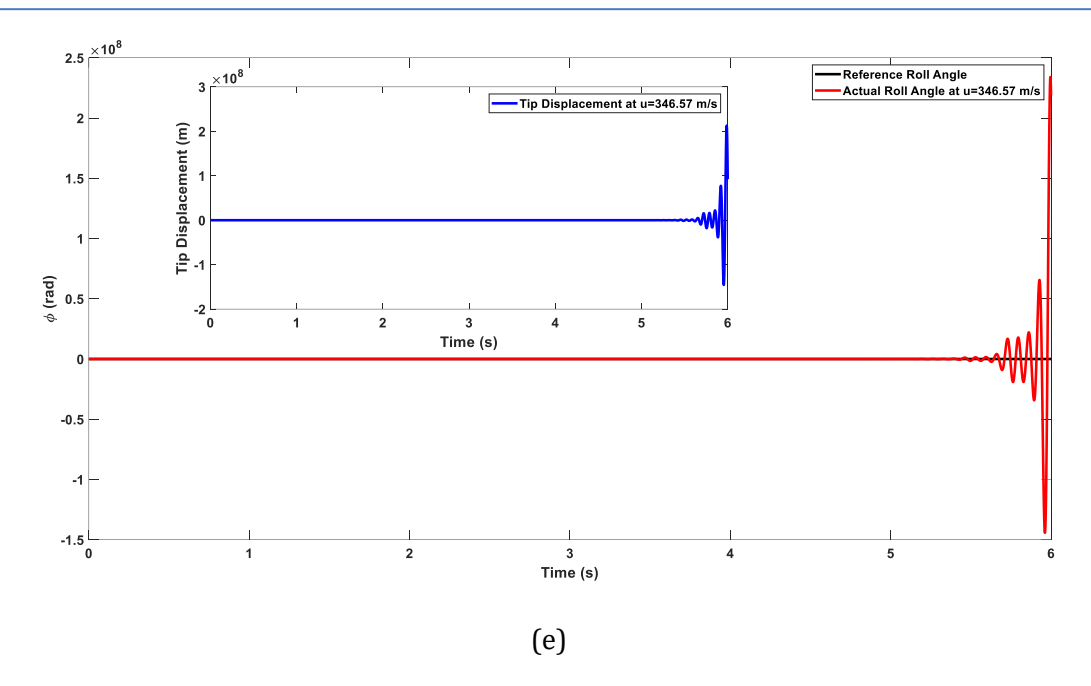


Fig. 9. The variation of roll angle of PD controlled quadrotor and displacement of pipe's tip at (a) u=63.01 m/s, (b) u=126.02 m/s, (c) u=252.05 m/s, (d) u=315.06 m/s, (e) u=346.57 m/s

As seen from the figures, the pipe vibrations between Figures 9a-9d are damped after a certain period of time despite the disturbing input. These vibrations, whose oscillation and damping period change depending on the fluid velocity, create different effects on the quadrotor. According to the results between Figures 9a and 9d, the amplitude of the pipe vibrations decreases with the increase in speed at changing speeds and the effect on the roll movement decreases as the fluid velocity increases. Pipe vibrations and roll angle show a more stable movement depending on the increase in fluid velocity. At lower fluid velocities, the amplitudes of the pipe vibrations increase and the moment forcing the roll angle to change increases. With the increase in moment, the roll angle makes larger angular movements. However, as seen, the changes in the roll angle while the quadrotor is fixed at a certain height are successfully controlled by the PD controller used. When the fluid velocity is 315.06 m/s, small amplitude oscillations are observed in the pipe, and it is observed that these oscillations continue continuously. This shows that the critical fluid velocity that will make the pipe vibrations unstable is now approached [35, 40]. When this critical speed is approached, the oscillations in the pipe also cause oscillations in the quadrotor roll angle. However, as the speed of the fluid in the pipe increases, the pipe vibrations show a continuously increasing trend. After the fluid speed exceeds 315.06 seconds, the pipe system becomes unstable and the large amplitude vibrations that occur also cause instability for the quadrotor. As seen in Figure 9e, when the fluid speed is 346.57 m/s, both the quadrotor and the pipe system lose their stability.

4.2. Test Scenario 2

In this scenario, a disturbance effect similar to the previous scenario was applied to the fluid conveying pipe. However, in this scenario, the response of the quadrotor to this disturbance input acting on the pipe during the control process was examined. As mentioned above, before the effect was applied to the pipe, both the z and Euler angles were waited to reach the desired reference values. Thus, the response of a quadrotor standing still in the air to the effect was observed. In this scenario, the disturbance effect was applied to the pipe after the quadrotor took off and before it reached the desired reference values. For this purpose, a unit step input was applied to the free end of the pipe for 0.1 seconds, starting at the 1.5th second of the movement. In this scenario, both the change in the roll angle of the quadrotor and the performance of the applied PD controller were examined. Figure 10 shows the disturbance input applied to the pipe.

In Figure 11, the variation of roll angle of the quadrotor under the input in Figure 10 is observed for different fluid velocities. The fluid velocity inside the pipe varies between 0 m/s and 346.57 m/s. This input between 1.5 and 1.6 seconds was applied until the roll angle of the quadrotor

reached the reference value of 1 rad. As can be seen from the figures in Figure 11, it takes approximately 3.2 seconds for the roll angle to reach the reference value without pipe vibration. For this reason, the desired effect was applied to the pipe in half of this settling time.

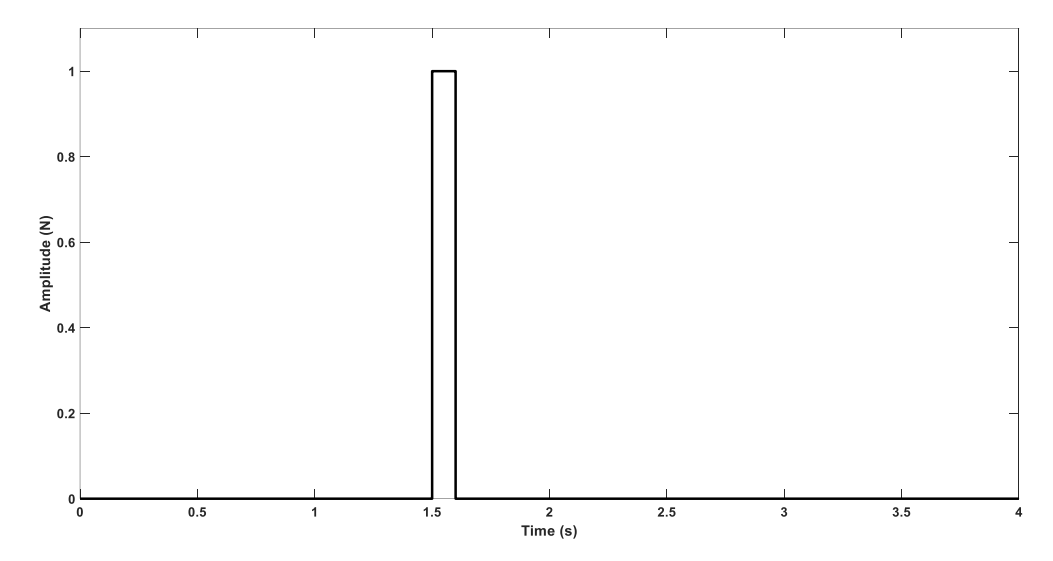
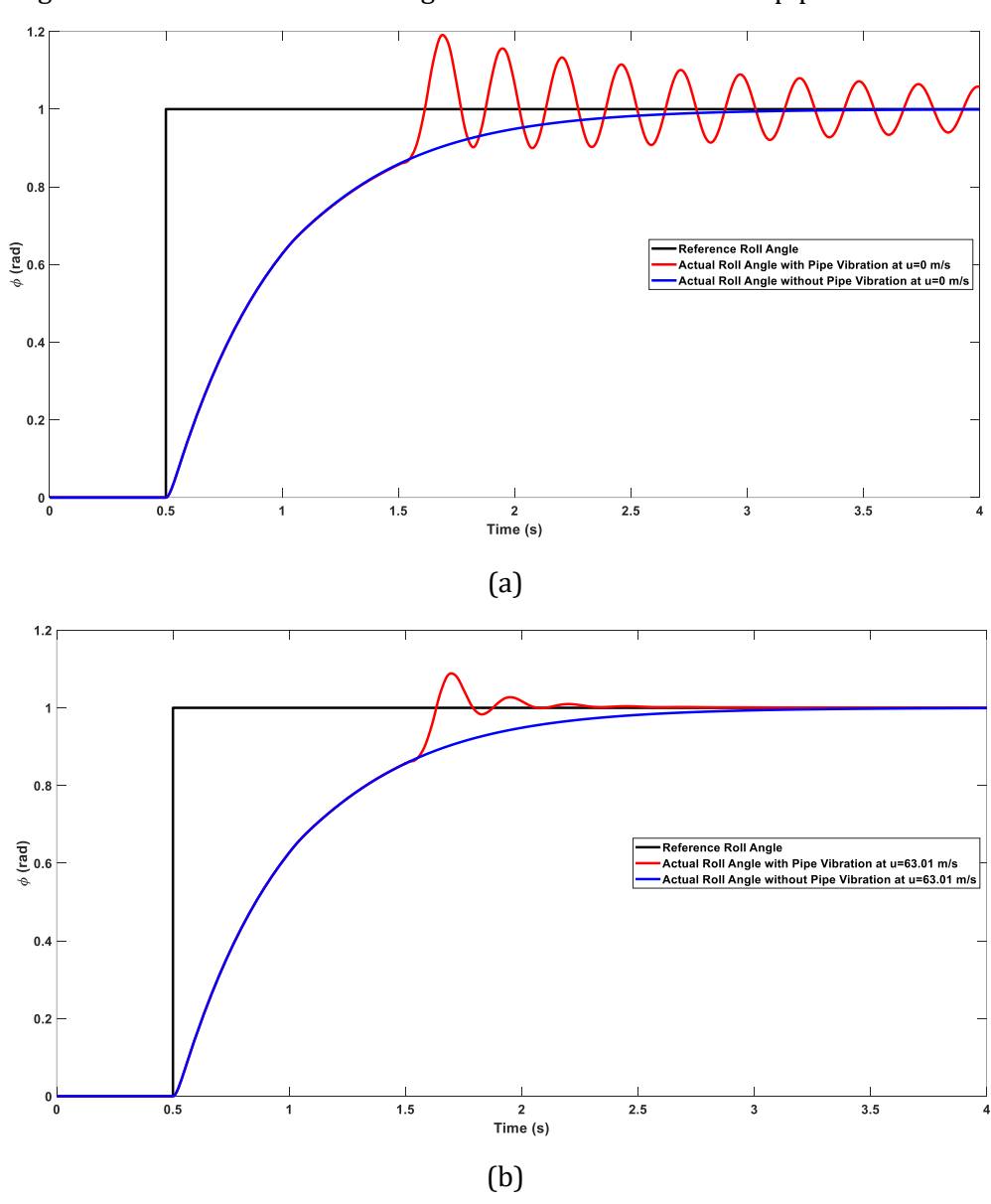


Fig. 10. The variation of the acting force at the free end of the pipe in Scenario 2



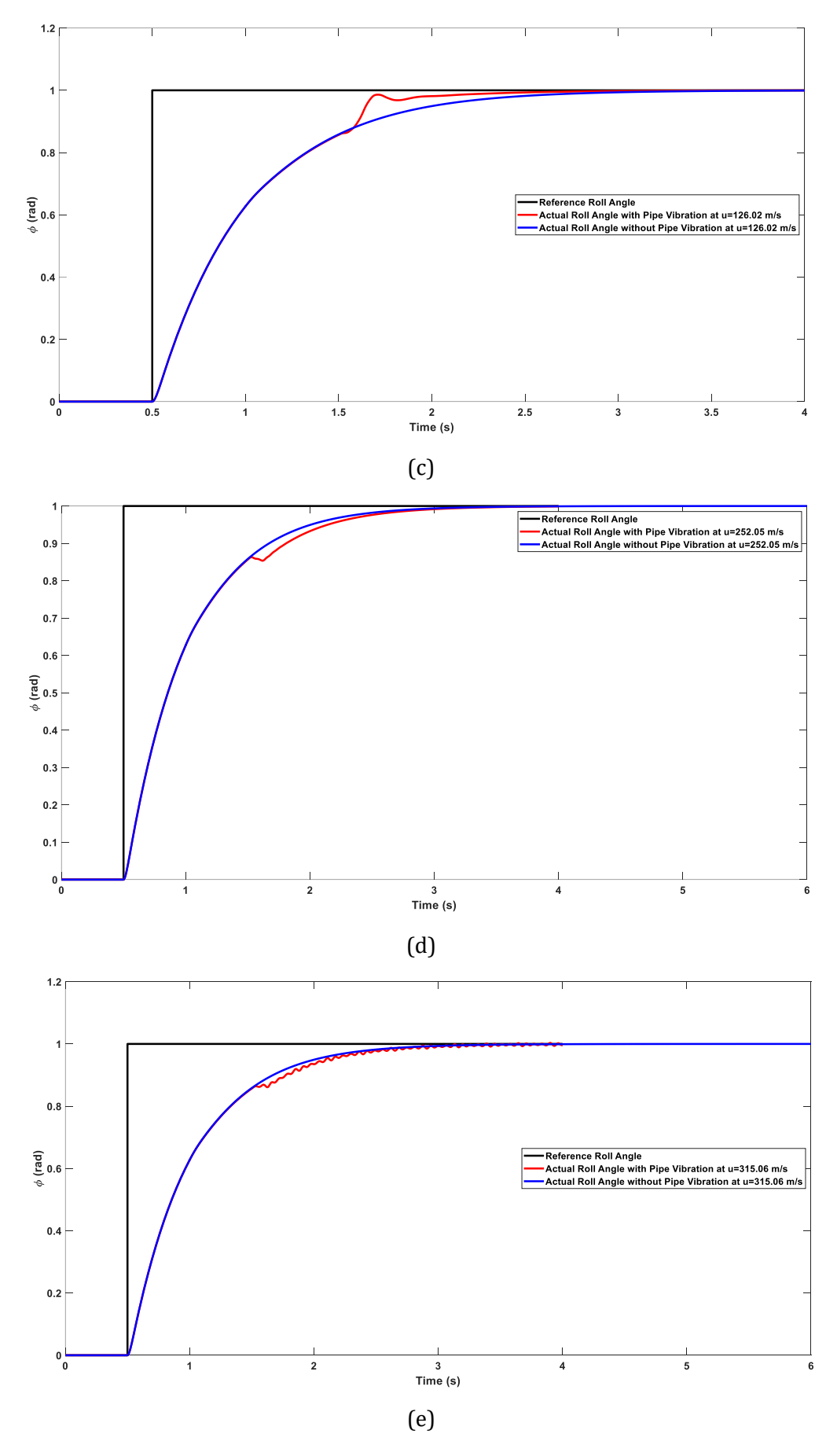


Fig. 11. Roll angle of PD controlled quadrotor under pipe vibration at a) u=0 m/s b) u=63.01 m/s, c) u=126.02 m/s, d) u=252.05 m/s, e) u=315.06 m/s

As can be seen from Figure 11, when the fluid velocity changes from 0 m/s to 315.06 m/s, the fluid conveying pipe and quadrotor maintain their stability. The PD controller has been successful in controlling the roll motion against pipe vibrations at all fluid velocities. When the disturbing effect is applied to the pipe, oscillatory changes in the roll angle are observed. When the fluid velocity is zero, there are oscillations around the reference value in the roll angle due to the oscillations in the pipe. In this case, it reveals the necessity of increasing the success of the PD controller used. In addition, by applying an additional control to the pipe, pipe vibrations can be eliminated or minimized, and it shows that significant decreases can occur in the vibration amplitude reaching the quadrotor. As in the previous scenario, the amplitudes of the pipe vibrations decrease as the fluid velocity increases, which causes less turning moment on the quadrotor. As seen in Figure 11b and Figure 11c, when the fluid speed is 63.01 m/s and 126.02 m/s, there is an upward change in the roll angle after t=1.5 s. This change, which is damped in time at these speeds, allows the roll angle to reach the reference value more quickly. As a result, the fluid speed in the pipe provides a positive contribution to the controller used at certain values and can ensure that the roll angle reaches the reference value earlier. From here, we can conclude that pipe vibrations at certain fluid speed ranges can contribute to the improvement of time domain criteria by helping the controller designed for the quadrotor. After a certain fluid speed, this effect reverses and the instability of the system increases again. As seen in Figure 11d, when the fluid speed is 252.05 m/s, the low amplitude oscillation in the pipe vibrations increases and can be structurally damped as in low speeds. The change in the roll angle shows that the PD controller is still successful, but it is observed that the settling time increases under the effect of pipe vibrations. In the previous scenario, when the fluid velocity is 315.02 m/s, it is observed that the vibrations in the pipe are small amplitude but continue as continuous oscillations. In this fluid velocity, like the previous scenario, small amplitude oscillations are observed after the effect is applied to the roll angle. For this scenario, tests with a fluid velocity greater than 315.06 m/s were not performed due to the instability of the pipe vibrations and the roll motion of the quadrotor.

4.3. Test Scenario 3

In this scenario, the change in the roll angle of the quadrotor was observed while the pipe was under a sinusoidal force. Unlike the previous scenarios, the reactions of both the pipe and the quadrotor to a disturbing input applied in a different form and for a longer period were examined. This type of disturbing effect may occur on the pipe under the influence of external factors such as weather conditions while the quadrotor is in the air. For this purpose, a force of $2*\sin(10t)$ N acts on the free end of the pipe. This force, like the previous case, was applied without reaching the roll angle reference value with the help of the controller. For this purpose, analyses were performed at different fluid velocities as a result of the disturbing force applied for 0.5 seconds between t=1.5 and t=2 seconds. The force acting on the free end of the pipe in this scenario is shown in Figure 12.

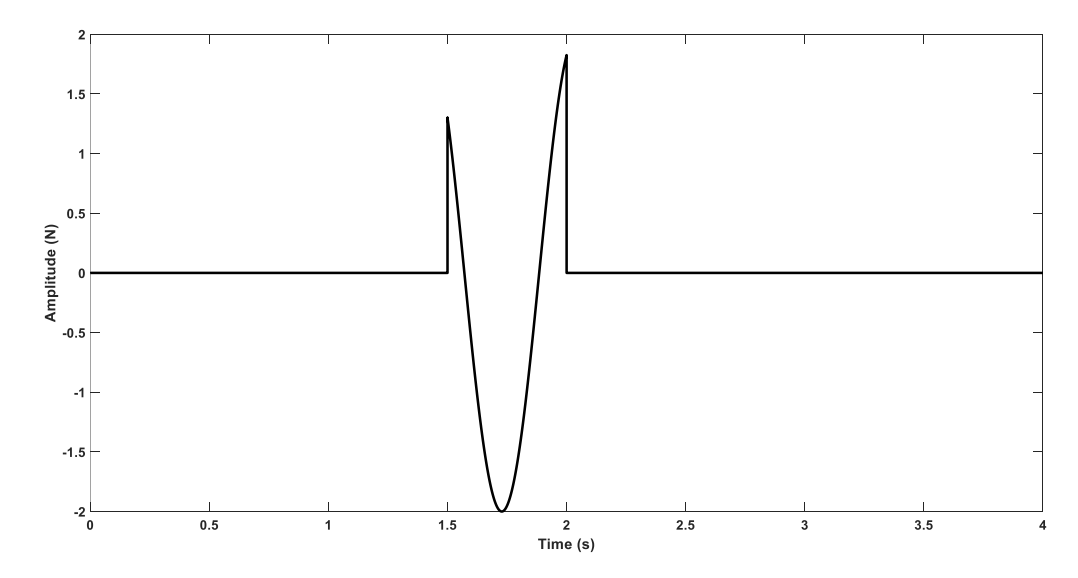
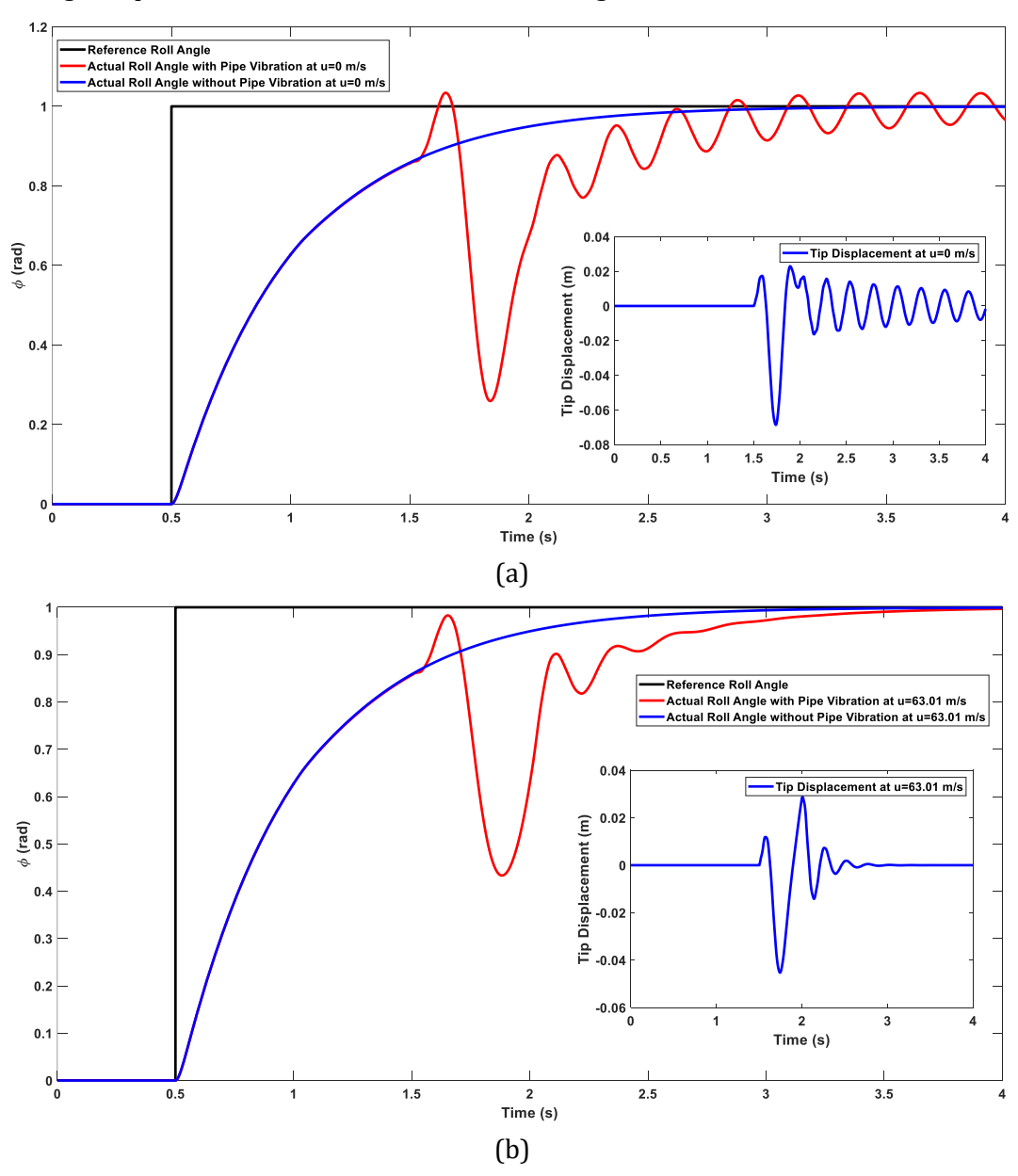


Fig. 12. The variation of the acting force at the free end of the pipe in Scenario 3

After this, the fluid conveying pipe vibrations and the change in roll angle corresponding to this disturbing input are investigated for different speeds. The control parameters of the PD controller used to control the roll angle of the quadrotor are the same for this scenario. Therefore, it takes approximately 3.2 seconds for the roll angle to reach the reference value of 1 rad without pipe vibrations. Figure 13 shows the pipe free end displacements and the roll angle changes caused by the moment caused by pipe vibrations on the quadrotor for the cases where the fluid speed varies between 0 m/s and 315.06 m/s.

As seen in Figure 13, the vibrations of the free end of the pipe are observed to be compatible with the sinusoidal input in terms of both increase and form. Depending on the input applied at t=1.5 sec, an increase in amplitudes was observed for type displacement and roll angle change. In addition, this input applied before the roll angle reached the reference value caused the angle change to fluctuate more than in the previous scenario from the moment it was applied. Especially, the formation of these high amplitude oscillations can be observed more clearly at low fluid speeds. As seen in the figures, the amplitude of the pipe vibrations reaches the levels of 0.004 m with the increase in fluid speed and continues to decrease until the critical speed is reached. This decreases the input effect of the quadrotor on the roll angle depending on the increase in fluid speed. The effect of the sinusoidal input applied for lower speeds in Figure 13b and Figure 13c is seen together with the high amplitude initial fluctuations in the roll angle.



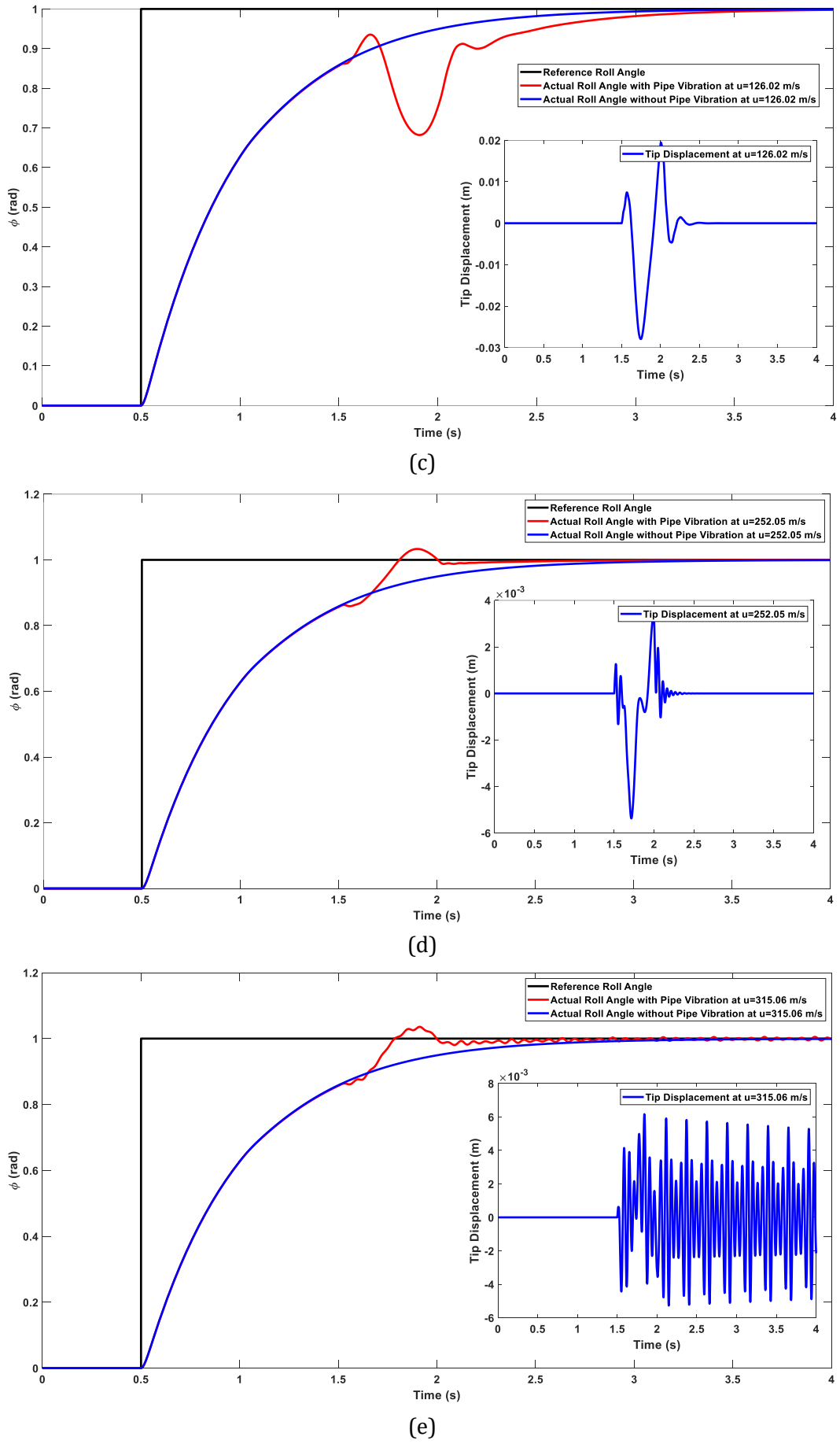


Fig. 13 The variation of roll angle of PD controlled quadrotor and displacement of pipe's tip at a) u=0 m/s b) u=63.01 m/s, c) u=126.02 m/s, d) u=252.05 m/s, e) u=315.06 m/s

This effect decreases significantly when the fluid speed reaches 252.05 m/s and 315.06 m/s as seen in Figure 13d and Figure 13e. This high amplitude angle change occurring at low fluid speeds also prolongs the time for the roll angle to settle to the reference value. It is observed that this time reaches 3.5 seconds when the fluid speed is 63.01 m/s and 126.02 m/s. For fluid speeds of 252.05 m/s and 315.06 m/s, a significant decrease is observed in the settling time due to the contribution of pipe vibrations. The settling time is around 2.5 seconds for both speeds. Despite the decrease in oscillation and the decrease in the settling time at high fluid speeds, an overshoot is observed in the change of the roll angle for 252.05 m/s and 315.06 m/s. This shows that the disturbance input, fluid speed and controller features are effective on the change of the roll angle.

5. Conclusion

In this study, the effects of fluid velocity and pipe vibration on the dynamic behavior of a quadrotor-fluid conveying vertical cantilever pipe system were investigated. A comprehensive system model was created to analyze quadrotor stability and pipe nonlinear vibrations by considering fluid-structure interaction and aeroelastic coupling. Euler method was used for the quadrotor model, and Euler-Bernoulli beam model based finite element method was used for modeling of the fluid conveying pipe. Both models were connected using the bending force and moment generated at the joint due to pipe vibrations. Observations were made under uncontrolled and PD control for the roll angle of the quadrotor, and no controller was applied for pipe vibrations. Then, tests were conducted at different fluid velocities and according to different pipe disturbance inputs.

According to the results obtained, it is shown that the fluid velocity and pipe excitation significantly affect the stability of the quadrotor and cause changes in the displacement of the free end of the pipe and the roll angle. It is observed that the amplitude of the pipe vibrations decreases with increasing the fluid velocity. However, this decrease continues until the fluid velocity reaches the critical level. For this reason, the roll angle of the quadrotor becomes more stable when the fluid velocity increases without exceeding the critical velocity. Therefore, the roll angle changes significantly at lower fluid velocities. However, when the critical fluid velocity is exceeded, both the pipe system and the quadrotor system lose their stability. When no control is applied to control the roll angle, the quadrotor behaves unstable for each fluid velocity. For this reason, in order to examine the effects of pipe vibrations more clearly, the U_2 force controlling the roll angle was controlled with the PD controller. It is seen that the performance of the PD controller is successful after the excitation applied before and after the roll angle settles at the desired reference value. In addition, the time domain criteria of the roll angle for the same inlet at different fluid velocities also vary. It has been determined that pipe vibrations occurring at certain speeds shorten the roll angle settling time to the reference value. This shows that pipe vibrations can provide positive contributions in the control phase. In addition, the type of distortion in the pipe significantly affects the rolling motion. When a sinusoidal-based disturbing input is applied, the roll angle follows this input and extends the settling time of the roll angle for low fluid velocities. For a 0.1 second step input, low fluid velocities shorten the settling time, and low fluid velocities lengthen the settling time for a 0.5 second sinusoidal input. As the fluid velocity increases, the settling time shortens by approximately 1 second, but the increase in the flow rate also causes an overshoot in the roll angle.

On the other hand, it has been observed that the PD controller applied yields successful results for different flow rates and drive types. As seen in this study, the use of such systems will increase and it is important to examine the interactions of the dynamics with each other in terms of efficiency. In addition, it has been determined that quadrotor-supported fluid transfer systems require optimized design and development of additional controllers for improved stability and performance. For this reason, it is planned to expand the system model of this study with future studies such as developing the quadrotor movement to affect pipe vibrations, adding an additional controller to the pipe to control pipe vibrations, preferring more adaptive controllers instead of PD controllers, and considering pipe vibrations in 3D.

Appendix

The element mass, gyroscopic and stiffness matrices are

$$M_{e} = \begin{bmatrix} \frac{13L(m+M)}{35} & \frac{11L^{2}(m+M)}{210} & \frac{9L(m+M)}{70} & \frac{-13L^{2}(m+M)}{420} \\ \frac{11L^{2}(m+M)}{210} & \frac{L^{3}(m+M)}{105} & \frac{13L^{2}(m+M)}{420} & \frac{-L^{3}(m+M)}{140} \\ \frac{9L(m+M)}{70} & \frac{13L^{2}(m+M)}{420} & \frac{13L(m+M)}{35} & \frac{-11L^{2}(m+M)}{210} \\ \frac{-13L^{2}(m+M)}{420} & \frac{-L^{3}(m+M)}{140} & \frac{-11L^{2}(m+M)}{210} & \frac{L^{3}(m+M)}{105} \end{bmatrix}$$
(A1)

$$G_{1} = \begin{bmatrix} \frac{12E^{*}I}{L^{3}} + \frac{13cL}{35} + MU \\ \frac{6E^{*}I}{L^{2}} + \frac{11cL^{2}}{210} - \frac{LMU}{5} \\ \frac{-12E^{*}I}{L^{3}} + \frac{9cL}{70} - MU \\ \frac{6E^{*}I}{L^{2}} - \frac{13cL^{2}}{420} + \frac{LMU}{5} \end{bmatrix}$$

$$G_{2} = \begin{bmatrix} \frac{6E^{*}I}{L^{2}} + \frac{11cL^{2}}{210} + \frac{LMU}{5} \\ \frac{4E^{*}I}{L} + \frac{cL^{3}}{105} \\ -\frac{6E^{*}I}{L^{2}} + \frac{13cL^{2}}{420} - \frac{LMU}{5} \\ \frac{2E^{*}I}{L} - \frac{cL^{3}}{140} + \frac{L^{2}MU}{30} \end{bmatrix}$$

$$G_{3} = \begin{bmatrix} \frac{-12E^{*}I}{L^{3}} + \frac{9cL}{70} + MU \\ -6E^{*}I + \frac{13cL^{2}}{420} + \frac{LMU}{5} \\ \frac{12E^{*}I}{L^{3}} + \frac{13cL}{35} + MU \\ -6E^{*}I - \frac{11cL^{2}}{210} - \frac{LMU}{5} \end{bmatrix}$$

$$G_4 = \begin{bmatrix} \frac{6E^*I}{L^2} - \frac{13cL^2}{420} - \frac{LMU}{5} \\ \frac{2E^*I}{L} - \frac{cL^3}{140} - \frac{L^2MU}{30} \\ -\frac{6E^*I}{L^2} - \frac{11cL^2}{210} + \frac{LMU}{5} \\ \frac{4E^*I}{L} + \frac{cL^3}{105} \end{bmatrix}$$

$$G_e = \begin{bmatrix} G_1 & G_2 & G_3 & G_4 \end{bmatrix}$$

$$K_1 = \begin{bmatrix} \frac{12EI}{L^3} + \frac{3g(m+M)}{5} - \frac{11M\dot{U}}{10} - \frac{6MUU_j}{5L} \\ & \frac{6EI}{L^2} - \frac{LM\dot{U}}{10} - \frac{MUU_j}{10} \\ -\frac{12EI}{L^3} - \frac{3g(m+M)}{5} + \frac{M\dot{U}}{10} + \frac{6MUU_j}{5L} \\ & \frac{6EI}{L^2} + \frac{gL(m+M)}{10} - \frac{MUU_j}{10} \end{bmatrix}$$

$$K_{2} = \begin{bmatrix} \frac{6EI}{L^{2}} + gL(m+M) - \frac{9LM\dot{U}}{10} - \frac{11MUU_{j}}{10} \\ \frac{4EI}{L} + \frac{gL^{2}(m+M)}{10} - \frac{L^{2}M\dot{U}}{10} - \frac{2LMUU_{j}}{15} \\ -\frac{6EI}{L^{2}} - \frac{LM\dot{U}}{10} + \frac{MUU_{j}}{10} \\ \frac{2EI}{L} - \frac{gL^{2}(m+M)}{60} + \frac{L^{2}M\dot{U}}{30} + \frac{LMUU_{j}}{30} \end{bmatrix}$$

$$K_{3} = \begin{bmatrix} \frac{-12EI}{L^{3}} - \frac{3g(m+M)}{5} + \frac{11M\dot{U}}{10} + \frac{6MUU_{j}}{5L} \\ -\frac{6EI}{L^{2}} + \frac{LM\dot{U}}{10} + \frac{MUU_{j}}{10} \\ \frac{12EI}{L^{3}} + \frac{3g(m+M)}{5} - \frac{M\dot{U}}{10} - \frac{6MUU_{j}}{5L} \\ -\frac{6EI}{L^{2}} - \frac{gL(m+M)}{10} + \frac{MUU_{j}}{10} \end{bmatrix}$$

$$K_{4} = \begin{bmatrix} \frac{6EI}{L^{2}} + \frac{gL(m+M)}{10} - \frac{LM\dot{U}}{5} - \frac{MUU_{j}}{30} \\ \frac{2EI}{L} - \frac{gL^{2}(m+M)}{60} + \frac{LMUU_{j}}{30} \\ \frac{-6EI}{L^{2}} - \frac{gL(m+M)}{10} + \frac{LM\dot{U}}{5} + \frac{11MUU_{j}}{10} \\ \frac{4EI}{L} + \frac{gL^{2}(m+M)}{30} - \frac{L^{2}M\dot{U}}{30} - \frac{2LMUU_{j}}{15} \end{bmatrix}$$

$$K_{4} = \begin{bmatrix} \frac{6EI}{L^{2}} + \frac{gL(m+M)}{10} - \frac{LM\dot{U}}{5} - \frac{MUU_{j}}{10} \\ \frac{2EI}{L} - \frac{gL^{2}(m+M)}{60} + \frac{LMUU_{j}}{30} \\ -\frac{6EI}{L^{2}} - \frac{gL(m+M)}{10} + \frac{LM\dot{U}}{5} + \frac{11MUU_{j}}{10} \\ \frac{4EI}{L} + \frac{gL^{2}(m+M)}{30} - \frac{L^{2}M\dot{U}}{30} - \frac{2LMUU_{j}}{15} \end{bmatrix}$$
(A3)

$$K_e = \begin{bmatrix} K_1 & K_2 & K_3 & K_4 \end{bmatrix}$$

where $m = M_{fluid}$ and $M = M_{nine}$.

(A2)

References

- [1] Ando H, Ambe Y, Yamaguchi T, Konyo M, Tadakuma K, Maruyama S, Tadokoro S. Fire Fighting Tactics with Aerial Hose-type Robot "Dragon Firefighter". IEEE International Conference on Advanced Robotics and its Social Impacts (ARSO), Beijing, China, 2019. https://doi.org/10.1109/ARSO46408.2019.8948716
- [2] Martinez-Guanter J, Aguera P, Aguera J, Pérez-Ruiz M. Spray and economics assessment of a UAV-based ultra-low-volume application. Precision Agriculture, 2020; 21:226-243. https://doi.org/10.1007/s11119-019-09665-7
- [3] Uddin SMM, Hossain MR, Rabbi MS, Hasan MA and Rahman Zishan MS. Unmanned Aerial Vehicle for Cleaning the High Rise Buildings. International Conference on Robotics, Electrical and Signal Processing Techniques (ICREST), Dhaka, Bangladesh, 2019. https://doi.org/10.1109/ICREST.2019.8644476
- [4] Nooralishahi P, Ibarra-Castanedo C, Deane S, López F, Pant S. Genest M, Avdelidis NP, Maldague XPV. Drone-Based Non-Destructive Inspection of Industrial Sites: A Review and Case Studies. Drones, 2021; 5(4): 106. https://doi.org/10.3390/drones5040106
- [5] Lee SM, Ng WH, Liu J, Wong SK, Srigrarom S, Foong S. Flow-Induced Force Modeling and Active Compensation for a Fluid-Tethered Multirotor Aerial Craft during Pressurised Jetting. Drones, 2022; 6(4): 88. https://doi.org/10.3390/drones6040088
- [6] Omar HM, Mukras SMS. Revolutionizing Palm Dates Harvesting with Multirotor Flying Vehicles. Applied Sciences, 2024; 14(22), 10529. https://doi.org/10.3390/app142210529
- [7] Ruiz JP, Toazo ER, Naranjo CA, Ortiz JS, Silva FM, Andaluz VH. Aerial Manipulator Robot Trajectory Tracking for Rhythmic Entertainment Applications. Proceedings of the Future Technologies Conference (FTC) 2024;4: 17-31. Springer, Cham. https://doi.org/10.1007/978-3-031-73128-0 2
- [8] Pasala HVS, Govindan N, Brahmbhatt S. Identification and Learning-Based Control of an End-Effector for Targeted Throwing. IEEE Robotics and Automation Letters, 2024; 9:11, 9558-9564, Nov. 2024. https://doi.org/10.1109/LRA.2024.3462250
- [9] Choi, YJ, Jung S. Experimental Studies on Solar Panel Cleaning Task by a Foldable Robot Arm of a Drone. Journal of Institute of Control, Robotics and Systems, 2023; 29(11): 887-892. https://doi.org/10.5302/J.ICROS.2023.23.0076
- [10] Raj DSS, Sethuraman TV, Shankar SS, Yashvanth VP, Perepu SK, Mohan S. An Autonomous Drone with Robotic End Effector for Maintenance Operation of 5G Mobile Towers. 3rd International Conference on Control and Robots (ICCR), 2020, Tokyo, Japan.
- [11] Suarez A, Vega VM, Fernandez M, Heredia G, Ollero A. Benchmarks for Aerial Manipulation. IEEE Robotics and Automation Letters, 2020; 5(2): 2650-2657. https://doi.org/10.1109/LRA.2020.2972870
- [12] Alberto J, Cervantes GS, Inanez CA, Mendez M. Air-arm: A new kind of flying manipulator. Workshop on Research, Education and Development of Unmanned Aerial Systems (RED-UAS). Cancun, Mexico, 2019.
- [13] Ramalepa LP, Jamisola RS. A Review on Cooperative Robotic Arms with Mobile or Drones Bases. International Journal of Automation and Computing, 2021;18:536-555. https://doi.org/10.1007/s11633-021-1299-7
- [14] Saunders J, Saeedi S, Li W. Autonomous aerial robotics for package delivery: a technical review. Journal of Field Robotics, 2024; 41: 3-49. https://doi.org/10.1002/rob.22231
- [15] Xiao LJ, Liu Q. Analysis of the deep sea mining pipe transverse vibration characteristics based on finite element method. Mathematical Problems in Engineering. 2021. https://doi.org/10.1155/2021/8216439
- [16] Kwag S, Eem S, Kwak J, Lee H, Oh J, Koo GH. Mitigation of seismic responses of actual nuclear piping by a newly developed tuned mass damper device. Nuclear Engineering and Technology. 2021; 53(8),:2728-2745. https://doi.org/10.1016/j.net.2021.02.009
- [17] Wu CJ, Jiao ZX, Xu Y., Hu JH, Pan H. Developments in pogo suppression methods for liquid rockets. Progress in Aerospace Sciences. 2023; 140: 100931. https://doi.org/10.1016/j.paerosci.2023.100931
- [18] Heng J, New T, Wilson P. Application of an Eulerian granular numerical model to an industrial scale pneumatic conveying pipeline. Advanced Powder Technology. 2019;30(2): 240-256. https://doi.org/10.1016/j.apt.2018.10.028
- [19] Païdoussis, MP, Issid, NT. Dynamic Stability of Pipes Conveying Fluid. The Journal of Sound and Vibration. 1974; 33: 267-294. https://doi.org/10.1016/S0022-460X(74)80002-7
- [20] Païdoussis MP, Li GX. Pipes Conveying Fluid: A Model Dynamical Problem. Journal of Fluids and Structures. 1993; 7: 137-204. https://doi.org/10.1006/jfls.1993.1011
- [21] Modarres-Sadeghi Y, Paidoussis MP, Semle C. Three-dimensional oscillations of a cantilever pipe conveying fluid. International Journal of Non-Linear Mechanics. 2008;43: 18-25. https://doi.org/10.1016/j.ijnonlinmec.2007.09.005
- [22] Liu ZY, Wang L, Sun XP. Nonlinear Forced Vibration of Cantilevered Pipes Conveying Fluid. Acta Mechanica Solida Sinica. 2018; 31: 32-50. https://doi.org/10.1007/s10338-018-0011-0

- [23] Li J, Deng H, Jiang W. Dynamic response and vibration suppression of a cantilevered pipe conveying fluid under periodic excitation. Journal of Vibration and Control. 2019;2511: 1695-1705. https://doi.org/10.1177/1077546319837789
- [24] Paidoussis MP. The dynamics of cantilevered structures subject to axial flow. Journal of Fluids and Structures. 2024;125: 104075. https://doi.org/10.1016/j.jfluidstructs.2024.104075
- [25] Semler C, Païdoussis MP. Nonlinear Analysis of the Parametric Resonances of a Planar Fluid-Conveying Cantilevered Pipe. Journal of Fluids and Structures. 1996;107: 787-825. https://doi.org/10.1006/ifls.1996.0053
- [26] Tang Y, Zhang HJ, Chen LQ, Ding Q, Gao Q, Yang T. Recent progress on dynamics and control of pipes conveying fluid. Nonlinear Dynamics. 2025; 113: 6253-6315. https://doi.org/10.1007/s11071-024-10486-1
- [27] Ibrahim RA. Overview of mechanics of pipes conveying fluids-Part I: fundamental studies. Journal of Pressure Vessel Technology. 2010; 132: 034001. https://doi.org/10.1115/1.4001271
- [28] Ibrahim RA. Mechanics of pipes conveying fluids-Part II: applications and fluid elastic problems. J Journal of Pressure Vessel Technology. 2011; 133: 024001. https://doi.org/10.1115/1.4001270
- [29] Païdoussis, MP. Fluid-Structure Interactions: Slender Structures and Axial Flow, Vol. 1. Academic, London,1998. https://doi.org/10.1016/S1874-5652(98)80003-3
- [30] Païdoussis, MP. Fluid-Structure Interactions: Slender Structures and Axial Flow, Vol. 2. Academic, London, 2004.
- [31] Pisarski D, Konowrocki R, Szmidt T. Dynamics and optimal control of an electromagnetically actuated cantilever pipe conveying fluid. Journal of Sound and Vibration. 2018; 432: 420-436. doi:10.1016/j.jsv.2018.06.045. https://doi.org/10.1016/j.jsv.2018.06.045
- [32] Szmidt T, Pisarski D, Konowrocki, R. Semi-active stabilisation of a pipe conveying fluid using eddy-current dampers: state-feedback control design, experimental validation. Meccanica. 2019; 54: 761-777. https://doi.org/10.1007/s11012-019-00988-3
- [33] Ikbal M, Kumar A, Jaya MM, Bursi OS. Vibration control of periodically supported pipes employing optimally designed dampers. International Journal of Mechanical Sciences. 2022;234: 107684. https://doi.org/10.1016/j.ijmecsci.2022.107684
- [34] Lin, YH, Chu CL. Active flutter control of a cantilever pipe conveying fluid using piezoelectric actuators. Journal of Sound and Vibration. 1996;1961: 97-105. doi:10.1006/jsvi.1996.0470. https://doi.org/10.1006/jsvi.1996.0470
- [35] Demir MH, Yesildirek A, Yigit F. Control of a cantilever pipe conveying fluid using neural network. 6th International Conference on Modeling, Simulation, and Applied Optimization (ICMSAO). Istanbul, Turkey,2015. https://doi.org/10.1109/ICMSAO.2015.7152198
- [36] Tsai YK, Lin YH. Adaptive modal vibration control of a fluid-conveying cantilever pipe. Journal of Fluids and Structures. 1997;11(5):535-547. doi:10.1006/jfls.1997.0092. https://doi.org/10.1006/jfls.1997.0092
- [37] Li J, Deng H, Jiang W. Dynamic response and vibration suppression of a cantilevered pipe conveying fluid under periodic excitation. Journal of Vibration and Control. 2019;25(11):1695-1705. https://doi.org/10.1177/1077546319837789
- [38] Zhang Y, Sun W, Zhang H, Du D, Xu K. Active vibration control of fluid-conveying pipelines: Theoretical and experimental studies. International Journal of Mechanical Science. 2024; 270: 109106. https://doi.org/10.1016/j.ijmecsci.2024.109106
- [39] Philip R, Santhosh B, Balaram B, Awrejcewicz J. Vibration control in fluid conveying pipes using NES with nonlinear damping. Mechanical Systems and Signal Processing. 2023; 194: 110250. https://doi.org/10.1016/j.ymssp.2023.110250
- [40] Yigit F. Active control of flow-induced vibrations via feedback decoupling. Journal of Vibration and Control. 2008; 14(4):591-608. https://doi.org/10.1177/1077546307082191
- [41] Ding H, Ji JC. Vibration control of fluid-conveying pipes: a state-of-the-art review. Applied Mathematics and Mechanics. 2023; 44: 1423-1456. https://doi.org/10.1007/s10483-023-3023-9
- [42] Bousbaine A, Wu, MH, Poyi GT. Modeling and Simulation of a Quad-Rotor Helicopter. University of Derby, UK 2021.
- [43] Iyer A, Bansal HO. Modelling, Simulation, and Implementation of PID Controller on Quadrotors. International Conference on Computer Communication and Informatics (ICCCI). Coimbatore, India, 2021. https://doi.org/10.1109/ICCCI50826.2021.9402301
- [44] Islam M, Okasha M, Idres MM. Dynamics and Control of Quadcopter Using Linear Model Predictive Control Approach. IOP Conf. Series: Materials Science and Engineering, 2017; 270: 012007. https://doi.org/10.1088/1757-899X/270/1/012007